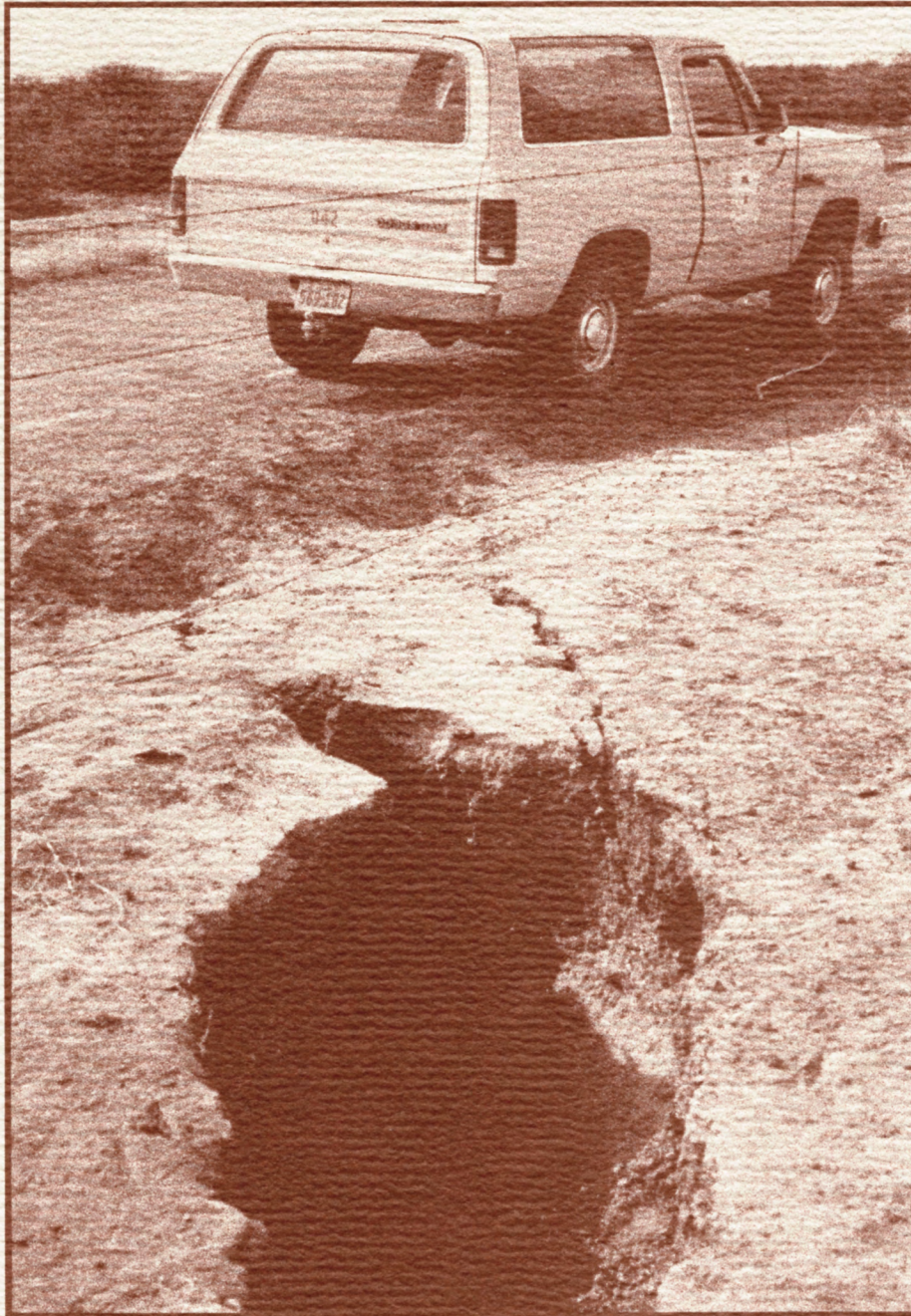


Geological Circular No. 92-2

Surface Fissures in the Hueco Bolson and Adjacent Basins, West Texas

Robert W. Baumgardner, Jr., and
Bridget R. Scanlon



Bureau of Economic Geology • W. L. Fisher, Director
The University of Texas at Austin • Austin, Texas 78713-7508 • 1992

Geological Circular No. 92-2

Surface Fissures in the Hueco Bolson and Adjacent Basins, West Texas

Robert W. Baumgardner, Jr., and
Bridget R. Scanlon

assisted by
Arten J. Avakian

Research funded by the Texas Low-Level
Radioactive Waste Disposal Authority under
Interagency Contract Number IAC(90-91)0268



Bureau of Economic Geology • W. L. Fisher, Director
The University of Texas at Austin • Austin, Texas 78713-7508 • 1992

Cover photograph:

Fissure formed in Ryan Flat south of Valentine, Texas,
on April 21 or 22, 1990. For further information,
see discussion in text beginning on page 29.

Contents

Abstract	1
Introduction	2
Terminology	2
Surface Fissures in the Western United States	2
Fissures Related to Ground-Water Withdrawal	5
Fissures Related to Natural Causes	5
Geologic Setting	6
Hueco Bolson	6
Paleoclimate	7
Study Area	7
Fissures in the Study Area	8
Surface Fissures	8
Fractures and Fracture Fill	11
Polygonal Fractures in the Petrocalcic Horizon	19
Subsurface Geologic Structure	19
Detailed Investigations in the Vicinity of Fissure 1	20
Quaternary Stratigraphy	20
Hydrology	21
Moisture flux	21
Ponding test	21
Other Fissures in the Region	26
Green River Valley	26
Quitman Canyon	26
Bolson El Cuervo	28
Eagle Flat	28
Salt (Wildhorse) Flat	29
Ryan Flat	29
Hueco Tanks	31
Discussion of Natural Fissure Development	31
Summary of Model	31
Tensional Stress and Localization of Fractures	33
Soil Piping	36
Surface Collapse	36
Summary of Fissure Development	36
Summary and Conclusions	37
Acknowledgments	38
References	38

Figures

1. Regional map of Quaternary faults and cross section of the Hueco Bolson	3
2. Location map of selected fissures reported in the western United States	4
3. Location map of three fissures and one relict fracture in study area	9
4. Map of fissure 1 and trenches	9
5. General view of southeast wall of trench 3 at fissure 1	13
6. Detail of fissure 1 in southeast wall of trench 3	14
7. Photographs of fracture showing parallel symmetry of fracture walls, trench floor, and clayey vertical laminae in fracture fill	16
8. General view of southeast wall of trench 4 at fissure 1	17
9. Detailed map of southeast wall of trench 4 at fissure 1	18
10. Bouguer gravity anomaly map of the Hueco Bolson study area	20
11. Profiles of sediment texture, gravimetric moisture content, water potential, chloride concentration, and moisture flux	22
12. Variation in volumetric moisture content with depth and time	23
13. Photograph of southeast wall of trench 3 below level of ponding test	24
14. Schematic cross sections of sediment texture, gravimetric moisture content, bromide concentration, and chloride concentration in soil samples	25
15. Map of fissures in region of the study area	27
16. Block diagrams depicting fissure evolution	32
17. Geologic settings of potential fissure development	33
18. Potentiometric surface map of southeastern Hueco Bolson	35
19. Schematic cross section of fissure 1	37

Tables

1. Characteristics of fissures and related factors reported in the southwestern United States	4
2. Fissures in desert basins of West Texas and northeast Chihuahua, Mexico	10

Abstract

Surface fissures have been observed in many desert basins in the western United States. These surface-collapse features are usually discovered after a normally dry surface has been covered with water, either by runoff from intense rainfall, by flooding, or by irrigation. Their sudden appearance attracts the attention of local residents, especially when the fissures render unpaved roads impassable. Collapse features begin as near-surface tension fractures that are enlarged by erosion and piping. Uneroded tension fractures are typically 0.1 to 7.6 cm wide and are filled with fine-grained sediment. Surface-collapse features may coalesce to form fissures, some up to 15 km long. Maximum reported depth of fissures or fractures is 25 m. Most tension fractures have formed where ground water has been pumped and water levels have dropped significantly (30 to 140 m). However, some fractures exist where no substantial pumping has occurred and no corresponding drop in water tables has been recorded. These features may have formed as a result of the lowering of ground water over geologic time. Tensional stress leading to fracture formation may result from differential compaction of unconsolidated sediments over bedrock irregularities or abrupt sedimentary facies boundaries or from desiccation. Seismic activity, although not a prerequisite for formation of collapse features, in some instances may trigger the development of tension fractures. Near-surface tension fractures may remain undetected until they are enlarged by piping and the surface above them collapses. Polygonal and branching patterns of fissures suggest desiccation as a cause of fracture genesis, but this origin remains unproven.

Fissures at the Hueco Bolson study area in western Texas are located on a flat-lying alluvial slope on Cenozoic sediments that fill a small basin in Cretaceous bedrock. The basin is separated from the main part of the Hueco Bolson by the Campo Grande fault. All three fissures at the Hueco Bolson study area are in topographic lows, indicating that overland flow is important to their development. The conditions necessary for piping to occur probably exist in the study area only in topographic lows during and after heavy rains.

Detailed study of fractures reveals that walls of fractures that underlie fissures match across each fracture's midline, evidence of simple tensional separation. These fractures are filled with silty, clayey sediment that contains vertical, clayey laminae, suggesting multiple periods of filling or fracturing or both. Fracture fill conducts water more readily than surrounding sediments, as seen at fissure 1. Low chloride concentrations down to 4.6 m below the surface near this fissure indicate that relatively high moisture fluxes occur there, compared with moisture fluxes in sediments in ephemeral stream channels and on low-lying interfluvies. Unlike in fissured areas elsewhere in the desert Southwest, there has been no significant ground-water pumping in the vicinity of the study area. However, four factors have led to lower ground-water levels in the study area over geologic time: incision of the Rio Grande, change to a warmer, drier climate, fault movement on the Campo Grande fault, and preferential drainage of relatively permeable basin fill beneath the study area. These fissures and those that form where ground water has not been pumped are natural geomorphic features of the desert Southwest.

Keywords: fissures, ground-water withdrawal, Hueco Bolson, hydrology, Quaternary stratigraphy, soil piping, subsidence, tension fractures, Trans-Pecos Texas

Introduction

This report describes surface fissures discovered in the Hueco Bolson of Trans-Pecos Texas, about 16 km northeast of the Rio Grande (fig. 1). The fissures are composed of holes and depressions aligned in discontinuous linear and curvilinear segments that locally overlap. These fissures formed by collapse of the surface above voids (soil pipes) that formed when near-surface sediments were washed into underlying tension fractures by percolating water.

This study of fissures was one facet of a geomorphic analysis of a site in Hudspeth County, Texas, that was being evaluated for use as Texas' repository for low-level radioactive waste. The presence of fissures at that location raised several questions about its suitability for long-term storage of radioactive waste: Did the fissures form as a result of seismic activity? Could they function as conduits between the surface and aquifers beneath the site? Was it likely that other fissures would form at the site? If so, could the time or place of their appearance be predicted? If a fissure formed beneath the waste repository, what effect would it have on movement of water below the repository?

These questions formed the core of this inquiry. To answer these questions, fissures at the site and elsewhere in the region were analyzed. Unfortunately, some results are inconclusive because critical data are unavailable or because similar features may result from different antecedent conditions. Nevertheless, the data support the following conclusions. First, the appearance of fissures is not evidence of local contemporaneous or preceding seismic activity. Second, fractures below fissures are more permeable than the surrounding near-surface sediments, but the fractures probably do not extend to the water table at the Hueco Bolson site. Third, fissures have formed in the past and will continue to form in the future, but when and where they might appear cannot be predicted with certainty.

Terminology

In the following discussion of fissures and fractures, a distinction is made between the fissure at the ground surface and the subsurface fracture that underlies it. The underlying fracture localizes the

formation of surface-collapse structures that compose the fissure. The fracture lies below the bottom of the shallow surface-collapse feature. The fissure is the surface feature composed of holes and depressions that form when surficial sediments collapse into horizontal soil pipes or are washed into the underlying fracture. Width and depth of the holes depends on the degree to which they have been eroded and filled with sediment. In profile, the bottom of the fissure is at the highest point of the fracture where horizontal opening of the fracture predominates over vertical collapse of sediment.

Surface Fissures in the Western United States

Surface fissures, reported in semiarid and arid regions of the western United States since the 1920's (Baker, 1927; Leonard, 1929), have been documented from southern California to western Texas and as far north as Idaho (fig. 2). The fissures described are typically linear and curvilinear collapse features (Schumann and others, 1986) that are segmented and overlap locally (Boling, 1986). The collapse features propagate upward and usually appear after irrigation, flooding, or runoff from intense rainfall has covered the ground surface (Underwood and DeFord, 1969; Holzer, 1976; Morton, 1977; Guacci, 1979; Boling, 1986; Larson, 1986; Larson and Péwé, 1986). Linear systems of fissures may be as much as 15 km long (Slaff, 1989) (table 1). Individual fissures as wide as 15 m and fractures as deep as 25 m have been observed (Boling, 1986; Slaff, 1989).

Fissures commonly form in unconsolidated sediments near margins of alluvial valleys or near outlying bedrock outcrops. Fissures adjacent to bedrock outcrops conform to the contact between alluvium and bedrock (Morton, 1977). They typically are oriented parallel or subparallel to the long axis of the host valley and approximately perpendicular to tributary drainage. As a result of this orientation they intercept runoff, which erodes the fissures into wide gullies. Because the fissures act as local catchment basins, the vegetation along them is generally more vigorous than elsewhere in the vicinity.

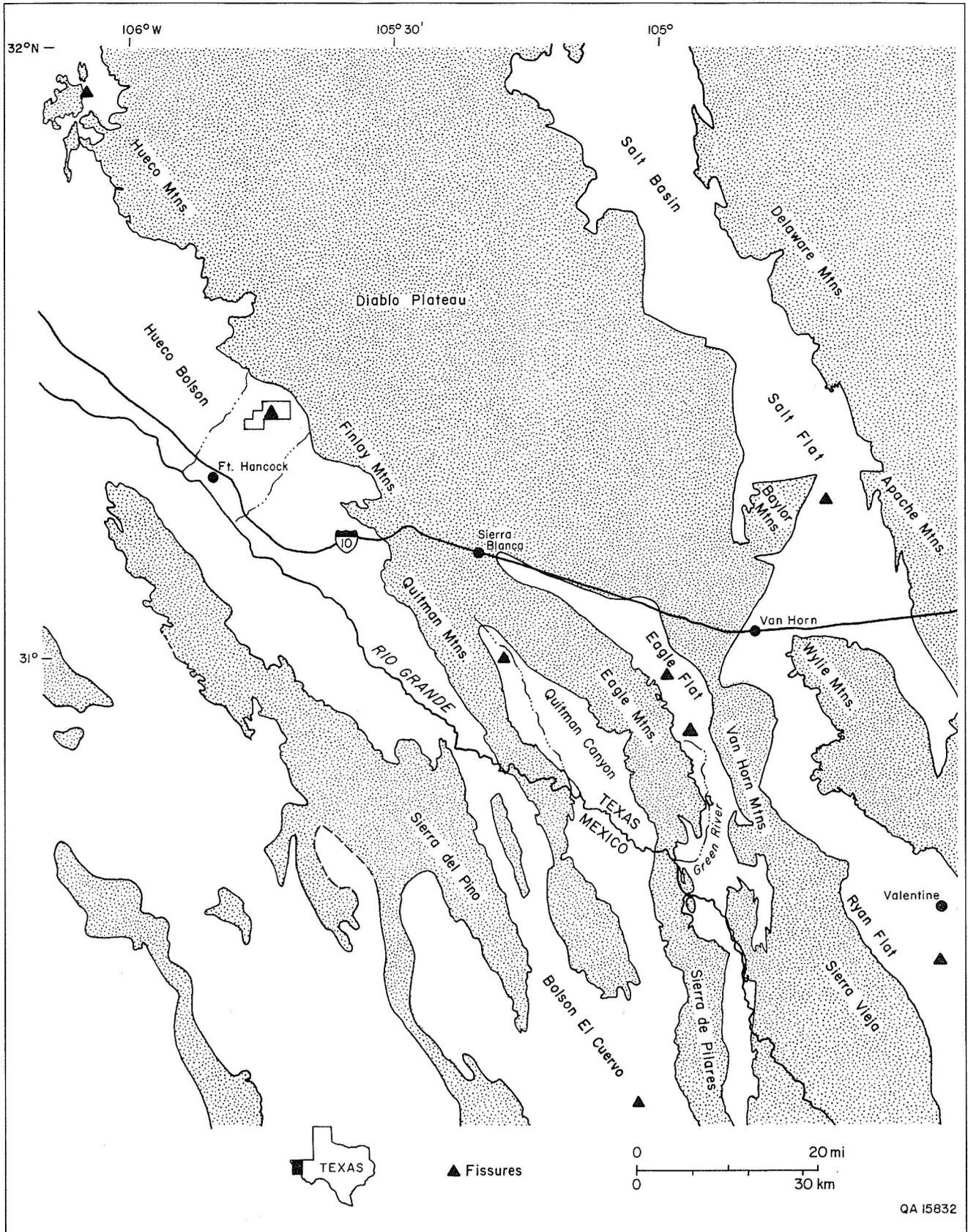


FIGURE 1. (a) Regional map of Quaternary faults in the Hueco Bolson, Trans-Pecos Texas. After Collins and Raney (1991, their fig. 1). (b) Cross section of the Hueco Bolson showing Quaternary and late Tertiary faults. After Raney and Collins (1990, their fig. 10).

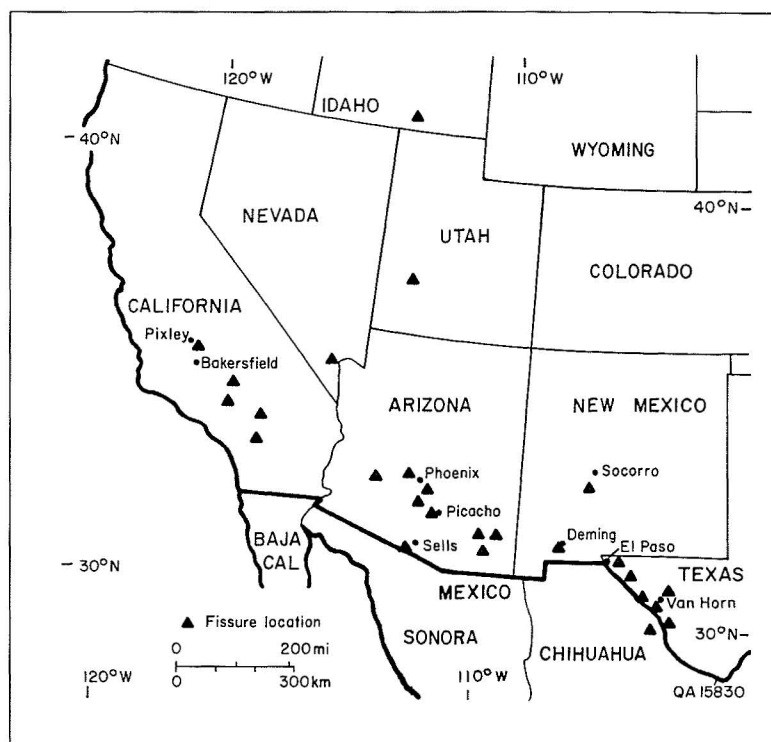


FIGURE 2. Location map of selected fissures reported in the western United States. After Robinson and Peterson (1962), Haenggi (1966), Schumann and Poland (1970), Underwood and DeFord (1975), Goetz (1977), Morton (1977), Guacci (1979), Jachens and Holzer (1982), Boling (1986), Larson (1986), Larson and Péwé (1986), Schumann and others (1986), Contaldo and Mueller (1988), and Haneberg and others (in press).

TABLE 1. Characteristics of fissures and related factors reported in the southwestern United States. (See fig. 2 for locations of fissures.)

Location	Fissure length (m)	Fracture		Ground subsidence (m)
		depth (m)	width (cm)	
South-central Ariz.	100's	25	0.1	—
Pixley, Calif.	800	>16.8	7.6	2.7
Central Ariz.	5,200	—	—	0.2
Phoenix, Ariz.	100's	≤20	—	2.0
Paradise Valley, Ariz.	120	≥3	—	1.5
San Jacinto Valley, Calif.	700	—	—	—
Santa Cruz Basin, Ariz.	1,000	≥20	2.5	3.8
Picacho Basin, Ariz.	15,800	≥4.6	—	—
Hueco Bolson, Tex.	140	>6	≤4.0	—

Location	Depth to bedrock (m)	Water table		Year first observed	Source
		Depth (m)	Drawdown (m)		
South-central Ariz.	50–300	—	100	—	1
Pixley, Calif.	1,800–2,100	14.6	40*	1969	2
Central Ariz.	—	—	—	1962	3
Phoenix, Ariz.	—	100	—	—	4
Paradise Valley, Ariz.	45	180	90	1980	5
San Jacinto Valley, Calif.	≤2,400	30	33	1953–74	6
Santa Cruz Basin, Ariz.	—	150	140	1927–?	7, 8
Picacho Basin, Ariz.	—	—	—	1927	9
Hueco Bolson, Tex.	200	110–180	—	1971–85	this study

Sources:

1 = Boling, 1986
2 = Guacci, 1979
3 = Holzer, 1976

4 = Larson, 1986
5 = Larson and Péwé, 1986
6 = Morton, 1977

7 = Schumann and Poland, 1970
8 = Schumann and others, 1986
9 = Slaff, 1989

*In confined aquifer at depth

Dash indicates that information was not available.

Fissures that have been excavated were reported to be underlain by fractures (Schumann and Poland, 1970; Guacci, 1979; Boling, 1986; Schumann and others, 1986). The fractures show some degree of opening, indicating a relative horizontal separation between the blocks on either side. Negligible vertical offset, persistent crack width with increasing depth, and simple horizontal separation of the blocks on either side of the fracture indicate that fractures are tensional breaks (Guacci, 1979; Schumann and others, 1986). The fracture may show evidence of episodic filling. Bull (1972) and Guacci (1979) described examples of fracture fillings consisting of discontinuous, vertical layers of varying types of sediment. Vertical layers lining fracture walls and in the center of the fracture fill and pockets of horizontal strata in the fracture fill suggest multiple periods of fracture filling and possibly fracture opening.

Some studies have addressed the relationship between fissure volume and fracture volume. Guacci (1979) estimated that the volume of the fracture beneath the Pixley, California, fissure might be large enough to accommodate the material lost from the fissure at the surface (Guacci, 1979). Holzer (1976) noted that cross-sectional areas of unfilled, upper parts of fissures in arid areas commonly exceed 3.5 m². In one example he estimated a fracture depth of 140 m, which was an average fracture width of 2.5 cm and which assumed that the volume of space between fracture walls was equal to the volume of material eroded from the fissure above. However, the deepest fracture reported in the literature on fissures (from another location) is only 25 m (Boling, 1986), which suggests that Holzer's (1976) estimated depth may be too large.

Fissure ages should be considered approximate. Fissures are usually reported only after they have become large enough to disrupt transportation or divert overland flow. Individual collapse features, too small to be observed on aerial photographs or to attract the attention of local residents, may exist for long periods before coalescing to form a fissure.

Fissures Related to Ground-Water Withdrawal

Earth fissures have developed extensively in areas of southern Arizona where land subsidence has resulted from ground-water withdrawal (Schumann

and others, 1986). Large-scale pumping of ground water in southern Arizona began about 1900 and increased in the late 1940's. The pumping has lowered water levels as much as 140 m, allowing compaction of silt and clay layers and resulting in subsidence. Aquifer compaction has occurred seasonally, mostly during summer periods when pumping and water-level decline are greatest. Ground-water withdrawal has resulted in compaction at depths greater than 253 m (Schumann and others, 1986).

Larson and Péwé (1986) reviewed literature on earth fissures and listed several mechanisms related to ground-water withdrawal that have been proposed to explain the origin of fissures, including (1) localized differential compaction of sediments, (2) shrinkage of dewatered sediments, and (3) regional differential compaction. They concluded that many fissures result from differential subsidence near buried bedrock hills or fault scarps. For example, an earth fissure in northeastern Phoenix, Arizona, formed over a convex-upward gravity anomaly, which was interpreted to indicate a bedrock hill with at least 30 m of relief that was buried 45 m deep. The top of the bedrock hill was at about the same depth as the original water level in the area. As the water level declined, differential compaction occurred in the sediments surrounding the buried hill.

Fissures Related to Natural Causes

Some fissures have formed in areas where there has been no substantial ground-water withdrawal, indicating that fissures can form by natural geomorphic processes in desert basins. An example of this type of fissure is the Picacho fissure, which formed on September 11 or 12, 1927, 4.8 km southeast of Picacho, Arizona, after a severe rainstorm (Leonard, 1929). Initially the fissure was about 300 m long, but it has since grown to 15.8 km long (Slaff, 1989). Its greatest measurable depth was 4.6 m. There was no apparent vertical displacement between the blocks on either side of the fissure, and development of the fissure was attributed to uneven settling of basin-fill material. Settling was thought to have been intensified by seismic shock of an earthquake that reportedly occurred on the evening of September 11, 1927, somewhere in the

southwestern United States or northern Mexico within about 320 km of the fissure. However, "no profound tectonic disturbance occurred in the Picacho area" (Leonard, 1929, p. 774).

Other fissures have formed in areas where ground-water pumping has not been extensive or before ground-water pumping began. Near Sells, Arizona, a fissure 0.8 to 1.2 km long was first observed in the early 1950's (Robinson and Peterson, 1962). At

that time, ground water was not used extensively for irrigation. Bull (1972) described other examples of cracks that formed in alluvial fans in California where no irrigation had occurred. He attributed their formation to compaction of moisture-deficient deposits. Surface water flowing across the surface of the fans wet the deposits adjacent to the channels, causing near-surface subsidence and cracking parallel to the channels.

Geologic Setting

Hueco Bolson

The Hueco Bolson is a fault-bounded basin in the Basin and Range province of Trans-Pecos Texas (fig. 1). The bedrock beneath the basin and exposed in the adjacent Diablo Plateau consists of Cretaceous and older sandstones and carbonates. The basin is filled by as much as 2,000 m of alluvium, which gradually thins to zero toward the northeastern margin (fig. 1b). The alluvium composes two formations: the Tertiary Fort Hancock Formation and Tertiary-Quaternary Camp Rice Formation (Albritton and Smith, 1965; Gustavson, 1991a). The Fort Hancock Formation is composed mostly of lacustrine and distal (fine-grained) alluvial-fan deposits. Sediments of the Camp Rice Formation were deposited unconformably over the Fort Hancock Formation beginning about 2.25 Ma ago, when the Rio Grande became a through-flowing stream (Gustavson, 1991a). In general, the Camp Rice Formation contains more sand and gravel than the Fort Hancock Formation, some of which was derived from source areas up river from the Hueco Bolson. However, clayey lacustrine deposits similar to those in the Fort Hancock also have been recognized in the Camp Rice (Gustavson, 1991a). Vertisols formed in these smectite-rich sediments. These paleosols are characterized by deep desiccation cracks, intersecting fractures with pedogenic slickensides, and mulch zones (Gustavson, 1991a). A 0.6-Ma-old volcanic ash deposit (Lava Creek B) at the top of the formation near El Paso, Texas, indicates that Camp Rice

deposition ended about 600,000 yr ago (Gile and others, 1981). The Camp Rice and Fort Hancock Formations are overlain by regionally extensive gravels deposited between successive periods of incision of the drainage system in the basin. The oldest (0.4 to 0.6 Ma) and topographically highest gravel, known as the Madden Gravel, caps the present-day interfluvies between arroyos. Younger gravels are present on lower terraces along the Rio Grande and along the arroyos (Albritton and Smith, 1965; Collins and Raney, 1991).

A well-developed (Stage III-IV) pedogenic calcrete is present in the Madden Gravel. The induration and the degree of cementation of this calcrete suggest that about 25,000 to 75,000 yr were required to form it (Gile and others, 1981). The calcrete, subsequently incised locally by arroyos and gullies and buried by alluvium, is now covered with a veneer of unconsolidated, weakly cemented sediments that are mostly less than 1 m thick in the study area.

Quaternary sediments in the immediate study area can be divided into four parts: a basal gravel, a middle silty sand unit, a strongly cemented upper sand or gravel, and an uppermost layer (locally absent) of silty, clayey sand. The basal gravel layer overlies fine-grained bolson sediments on an abrupt, irregular contact. Thickness of the gravel layer ranges from about 0.5 to 2.4 m. The gravel is interpreted as coarse channel-fill deposits of braided streams. The middle sand unit contains low-angle crossbeds locally, evidence of fluvial deposition. A strongly cemented silty sand or gravel overlies the middle

sand. Locally, two carbonate-cemented (petrocalcic) horizons are present within 5 m of the surface. These calcretes, separated by sediments deposited when streamflow probably was more frequent than it is now, represent two different periods of landscape stability.

The upper calcrete is overlain by unconsolidated sediments of the fourth and youngest component of the Quaternary sequence. These strata have radiocarbon ages ranging from $1,440 \pm 80$ yr B.P. to $7,510 \pm 110$ yr B.P. (corrected for $\delta^{13}\text{C}$). The oldest dated sediments overlying the upper petrocalcic horizon in the study area have a radiocarbon age of $7,510 \pm 110$ yr, which approximately corresponds to the onset of modern climatic conditions about 8,000 yr ago, as reported by Van Devender and Spaulding (1979). Most of the Quaternary sediments that overlie the upper petrocalcic horizon at the study area have accumulated within the last 7,500 yr under climatic (and probably hydrologic) conditions similar to those that prevail at present. However, the sediments did not accumulate uniformly or without interruption. The gravelly channel-fill deposits in these strata demonstrate that deposition and erosion occurred episodically throughout this period. Furthermore, they suggest that erosion was also occurring downslope on the main arroyos near the study area.

Since the end of Camp Rice deposition in middle Pleistocene time, the Rio Grande has incised the bolson fill, possibly in response to a drop in base level caused by climatic changes related to global glacial cycles (Gile and others, 1981). The evidence of cyclic stability and incision by the Rio Grande is the "stepped sequence of graded surfaces located between the valley floors and the . . . piedmont slopes" in southern New Mexico (Gile and others, 1981, p. 48). In the study area, surfaces probably equivalent to those described in southern New Mexico are found within the valleys of the major arroyos (Collins and Raney, 1991).

On the basis of similarities in radiocarbon ages from the study area and the Organ geomorphic surface in southern New Mexico, and of similarities in their positions relative to other geomorphic surfaces, the study area is interpreted to be on the Organ geomorphic surface. This surface is the youngest major depositional surface of the post-Camp Rice sequence (Gile and others, 1981). The bulk of Organ alluvium accumulated between 6,400 and 2,200 yr B.P. (Gile and others, 1981). Similarly,

most alluvium above the petrocalcic horizon at the study area accumulated between about 7,510 and 1,440 yr B.P.

According to Gile and others (1981), valley filling and cutting during the Quaternary were controlled by climate. Climatic fluctuations and cyclic downcutting on the Rio Grande would have affected water levels in the bolson fill. Downcutting and the resulting drop in base level lowered water levels (Gile and others, 1981); higher water tables probably prevailed during periods of wetter climate. However, no evidence has been found to suggest that water tables were shallow enough to affect soil development (Gile and others, 1981).

Paleoclimate

During the Wisconsinan Full-Glacial Period, about 25,000 to 14,000 yr ago, the climate of the southwestern United States was cooler and moister than it is currently (Hall, 1985). In the Late Glacial Period, 14,000 to 10,000 yr ago, climatic conditions became warmer and drier (Hall, 1985), and there was a transition from glacial to postglacial vegetation throughout the Southwest. At about the same time, entrenchment of the Rio Grande occurred (Hawley and Kottowski, 1969). Xeric woodlands of juniper or juniper and oak persisted until about 8,000 to 5,000 yr ago, when woodland species in the lowlands were replaced by grass, and present-day climate and vegetation were established in the deserts of the Southwest (Van Devender and Spaulding, 1979; Horowitz and others, 1981; Markgraf and others, 1984). Between 1,700 and 1,500 yr ago, soils were eroded and desert shrub was established (Van Devender and Spaulding, 1979). This period of soil erosion may be represented in the study area by the sharp contact at the base of a soil horizon that has a radiocarbon age of $1,440 \pm 80$ yr.

Study Area

The study area lies on an alluvial slope above a small closed subbasin between the Diablo Plateau to the east and the main part of the Hueco Bolson to the west (fig. 1b). The subbasin is separated from the main part of the bolson by the northwest-striking Campo Grande fault, which parallels the edge of

the Diablo Plateau (fig. 1). Evidence of several episodes of normal faulting on the Campo Grande fault in the last 500,000 yr (Collins and Raney, 1991) suggests that the Hueco Graben (fig. 1) continues to subside relative to the Diablo Plateau. Depth to Cretaceous bedrock beneath the study area, based on core from boreholes, is as much as 217 m.

Composed primarily of low-relief interfluvial and shallow (mostly less than 60 cm deep) drainageways of ephemeral streams, the surface of the study area slopes to the southwest at about 10 m/km. Major streams near the area are incised as deeply as 20 m, locally exposing Camp Rice and Fort Hancock Formations in valley walls and arroyo floors.

Surface and near-surface sediments, which are predominantly sandy, were deposited by ephemeral streams crossing the alluvial slope. Soils are mostly loam and fine sandy loam over fine sandy loam, loam, or clay loam (Allen, 1990). Coppice dunes, composed mostly of silty fine sand, are present locally. Commonly 1 m high and 5 m long, these vegetation-covered dunes range up to 1.5 m high

and 10 m long. Gravel also is locally abundant in erosion-resistant deposits that crop out to form topographic highs with local relief of 0.5 to 3 m. These highs probably are lenses of gravel that were originally deposited in the bottoms of ephemeral stream channels. Near-surface sediments (<3 m deep) range from gravelly, muddy sand to muddy sand, and some sandy silt and sandy mud, as defined in the Folk (1974) classification.

There has been no significant ground-water withdrawal at the study area for either agricultural or domestic use. Ground water in the Hueco Bolson aquifer flows from the Diablo Plateau toward the Rio Grande (Mullican and Senger, 1990). Depth to ground water varies from 110 to 180 m (Mullican and Senger, 1990). No recent decline in water levels has been documented in wells near the study area, which are pumped by windmills and used primarily for filling small stock tanks. The nearest irrigated fields are 16 km away on the floodplain of the Rio Grande, supplied with water from the alluvial aquifer of the Rio Grande.

Fissures in the Study Area

Three surface fissures ranging from 20.5 m (fissure 2) to 140 m (fissure 1) long and one relict fracture have been found in the study area northeast of Fort Hancock, Hudspeth County, Texas (fig. 3). The fissures overlie fractures, which extend from the base of the fissure to some depth below the surface. Small pits were dug by hand to the top of the petrocalcic horizon at all three fissures. Deeper trenches were excavated across fissure 1 (fig. 4), allowing detailed description of this fissure and the fracture beneath. The relict fracture, with no fissure above it, was exposed in the floor and walls of a 6-m-deep trench and is at least 30 m long (the width of the trench in which it is exposed). This fracture is filled with sediment, suggesting that at one time a fissure formed above as sediment collapsed to fill the fracture. The fissure has been obscured or removed by subsequent erosion and deposition or bioturbation of alluvium above the fracture.

Surface Fissures

The surface fissures in the study area are composed of aligned surface-collapse features and soil pipes, which are roughly slot to wedge shaped and straight walled or narrow downward in profile. Maximum depth of collapse features is 135 cm; maximum width is 157 cm. Both maxima were seen at the longest fissure (fissure 1). At fissures 2 and 3, collapse features are about 55 to 60 cm deep. Most collapse features at fissure 1 are about 1 m deep and less than 1 m wide. Width/depth ratios of the fissures, which increase as they are eroded and filled with sediment, range from 0.2 to 2.0 (table 2). The collapse features are discontinuous, separated by bridges of sediment over horizontal soil pipes. Locally, up to 10 m of uncollapsed material lies between these holes (fig. 4), but spacing between them is more commonly 1 to 3 m.

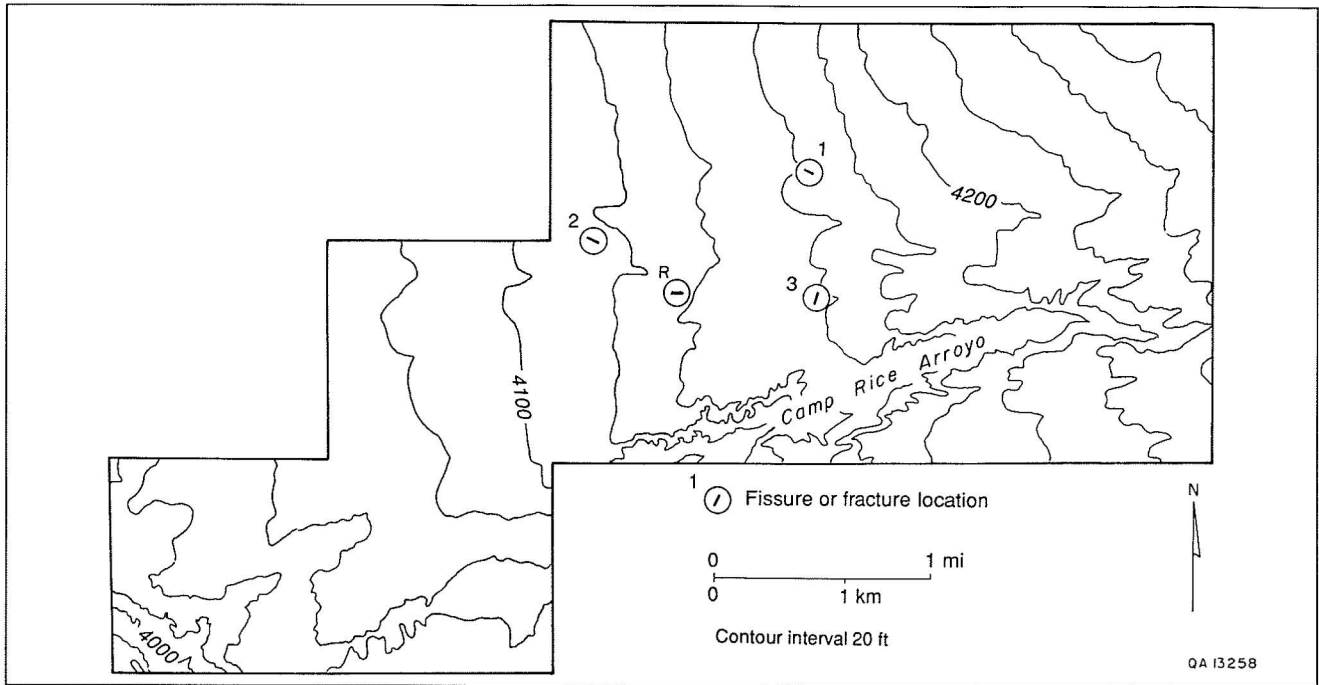


FIGURE 3. Location map of three fissures (1, 2, 3) and one relict fracture (R) found in study area. Fissure numbers are referred to in the text. Line within each circle represents orientation of that feature (length not to scale). Orientations are fissure 1 = 305°, fissure 2 = 310°, fissure 3 = 20°, relict fracture = 85°. No collapse features are present at the surface above the relict fracture (the fracture was exposed in a 6-m-deep trench). See figure 1 for map location.

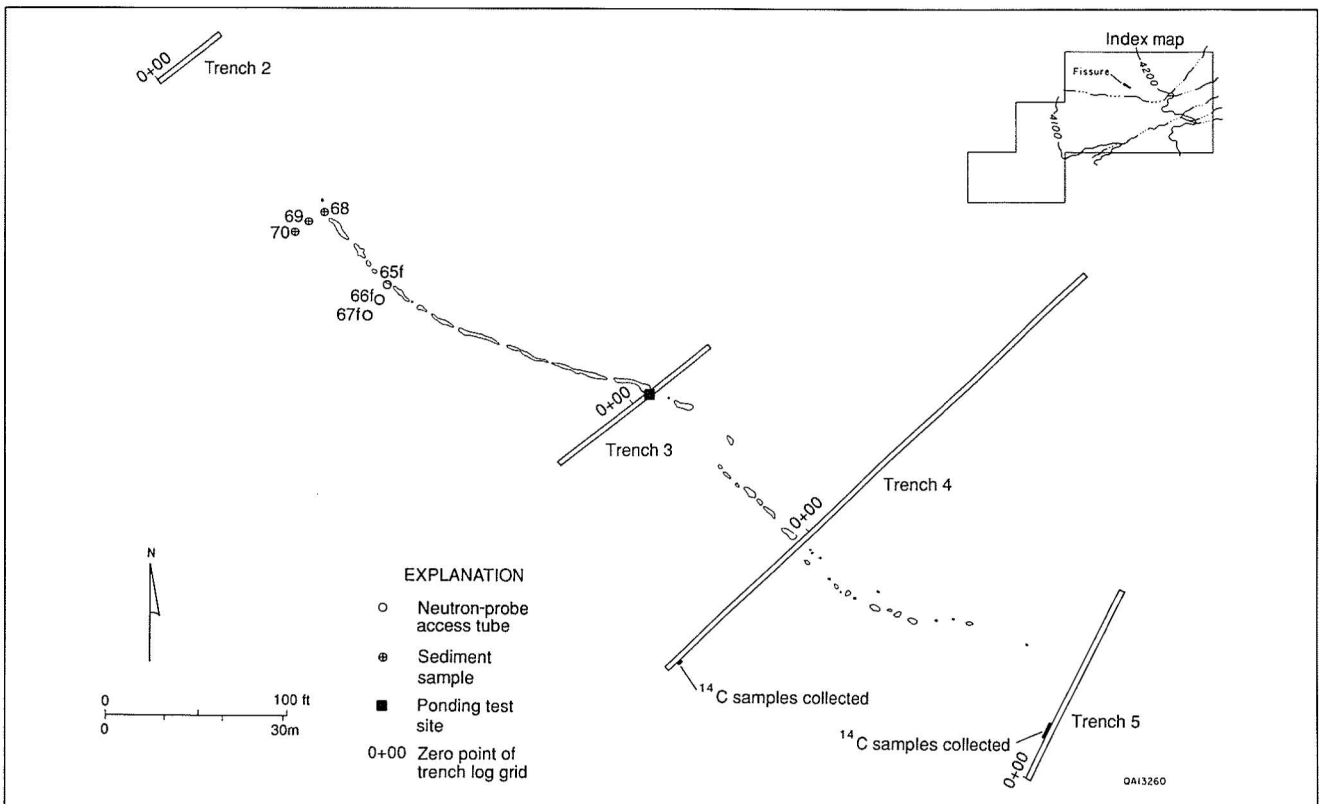


FIGURE 4. Map of fissure 1 and trenches, showing locations of sampled boreholes, neutron-probe access tubes, and site of ponding test. Trench 1 (not shown) is about 30 m northwest of trench 2. After Sergent, Hauskins and Beckwith (1989, their fig. 7).

TABLE 2. Fissures in desert basins of West Texas and northeast Chihuahua, Mexico. See figure 15 for locations of fissures.

Location	Length (m)	W/D ratio	Geologic unit	Date first observed	Source
Bolson El Cuervo	—	—	bolson deposits	pre-1965	5, 8
Eagle Flat	65	0.4	alluvium	?	8, 9
Eagle Flat	—	2.7	alluvium	post-1927/28	8, 9
Eagle Flat	910	28	alluvium	1927 or 1928	8, 9
Green River valley	740	~0.5 ¹	bolson deposits	pre-1927, 1959	2, 9
Hueco Bolson	140	0.2 to 2	alluvium	1971-1985	this study
Hueco Tanks	190	0.25 ¹	alluvium	9/11-9/14/90	6
Hueco Tanks	750	—	alluvium	pre-1942	this study
Quitman Canyon	4,200	0.2 to 5	alluvium	1924	1, 9
Quitman Canyon	200	—	alluvium	pre-1957	this study
Quitman Canyon	305	~1.2 ¹	alluvium	1985	7
Ryan Flat	>500	0.1	alluvium	4/20-4/21/90	this study
Salt Flat	800	—	lacustrine deposits	pre-1946	3, 4

Location	UTM coordinates ²		USGS topographic map (7.5-min. quadrangle)
	Easting	Northing	
Bolson El Cuervo	unknown	unknown	n/a
Eagle Flat	501000	3426600	Bass Canyon
Green River valley	505500	3419200	Bass Canyon
Hueco Bolson	430100	3475000	Diablo Canyon West
Hueco Tanks	397300	3531300	Hueco Tanks
Quitman Canyon	471700	3428500	Cedar Arroyo
Ryan Flat	549400	3373900	Deer Peak
Salt Flat	527000	3455900	Watson Ranch

Sources: 1 = Albritton and Smith, 1965 4 = Goetz, 1985 7 = Sergent, Hauskins and Beckwith, 1989
 2 = Baker, 1927 5 = Haenggi, 1966 8 = Underwood and DeFord, 1969
 3 = Goetz, 1977 6 = Moss, written communication, 1990 9 = Underwood and DeFord, 1975

¹Width/depth (W/D) ratio as reported by source. All others were measured in the field in 1989.

²All Universal Transverse Mercator (UTM) coordinates are in zone 13. Coordinates are for the center of a fissure network or for the largest network having several discrete ones.

Dash indicates that information was not available; n/a indicates that information was not applicable.

The widest and longest collapse features are near the middle of fissure 1, and the smallest collapse features are near the northwest and southeast ends of the fissure (fig. 4). Assuming that the largest collapse features are the oldest because they have been eroded more by overland flow, the fissure appears to have propagated laterally away from an origin near its center. Fissure 1 is composed of two, or possibly three, arcuate segments. The two principal segments overlap slightly between trenches 3 and 4 (fig. 4). The southeast segment may be composed of two smaller segments that overlap a few meters southeast of trench 4.

Several lines of evidence indicate that overland flow is critical to fissure development and filling. All fissures in the study area are in topographic

lows where runoff is concentrated during rainstorms. At fissures 1 and 3, leaf litter and branches have washed into the collapse features, evidence that the fissures capture runoff when it occurs. There are small, uncommon accumulations of gravel in fissure 1, probably derived locally from the ground surface or eroded from the fissure wall. Fissure 3 extends upslope beyond the topographic low where the vegetation cover is relatively thick. On the less-vegetated slope, grasses and forbs are more common within 2 m of the fissure than farther away, indicating that moisture content of the soil near the fissure occasionally is high enough to enhance growth of annual plants. Runoff captured by the fissure in the topographic low may move laterally through the fissure system to points outside that low.

Although surface runoff appears to be necessary for development of the fissures, the orientation of fissures is independent of the direction of overland flow. Fissure 1 trends 305°, oblique to local drainage, and lies in a topographic low that has about the same orientation. Fissure 2 is oriented about 310°, subparallel to the topographic low that it is in. Fissure 3 is a curvilinear feature that is roughly perpendicular to drainage. Its orientation, measured end to end, is 20°.

Fractures and Fracture Fill

At the study area, all known fissures are underlain by near-vertical fractures that are subparallel to surface-collapse features (for example, fig. 5). Widths of 2 to 4 cm are typical of all fractures, including the relict one. The fracture at fissure 1 narrows downward irregularly from a maximum of 6.5 cm at a 3.8-m depth to 2.5 cm at a 5.6-m depth (fig. 6). Maximum width of the fracture in the top of the petrocalcic horizon at fissure 2 is 7 cm. These greater widths may result from widening of the tensional fracture by local erosion and collapse of the walls. In contrast, where their walls have eroded little and display parallel symmetry (walls of fracture are parallel across the fracture), fractures are typically narrower (3 to 4.5 cm wide).

The fracture below fissure 1 is at least 6.2 m deep, the maximum depth of trench 3 (fig. 6). The relict fracture is exposed to a similar depth. Both fractures extend to greater depths. If one assumes downward movement and storage within the fracture of all material removed from the widest collapse feature at the surface (which has a cross-sectional area of 9,000 cm²), a fracture 2.5 cm wide would need to be 36 m deep to accommodate the same amount of sediment. This approach may overestimate the depth of the fracture, because some of the sediment missing from the collapse feature may have been compacted by wetting or may have been flushed out of the fracture and into porous gravel layers that the fracture intersects (fig. 6). Furthermore, such a large depth estimate may be unreasonable because overburden pressure may cause the fracture to terminate at a depth shallower than that estimated by the calculations. In fact, there is some evidence for a shallower depth. First, if the fracture below a 5.6-m depth narrows by the same percentage/unit depth (50 percent/1.46 m) that it does between

3.8 m and 5.6 m, then the crack should terminate at about 8.5-m depth [$5.6 \text{ m} + (2 \times 1.46 \text{ m}) = 8.5 \text{ m}$]. Second, the fracture at fissure 1 branches downward and deviates from vertical, and each branch is smaller than the main fracture (fig. 6). One branch appears to die out downward at 5.8 m (fig. 6) in trench 3.

There is no evidence of faulting at fissure 1 or at the relict fracture. (The fractures are not exposed below the calcrete at fissures 2 and 3, so no observations of the fracture walls there were possible.) The fracture has opened only by a horizontal separation of the fracture walls caused by tensional forces. Where the fracture walls are not eroded or modified by localized collapse, they match straight across the fracture (fig. 7a). Simple tensional separation of the fracture walls also is seen where the fracture locally branches and rejoins, enclosing pieces of silty sand and carbonate-cemented gravel (fig. 6, 5.5-m and 3-m depths, and fig. 7b). These enclosed pieces have not rotated and therefore are additional indications of simple tensional cracking.

The fractures are filled primarily with sediment ranging from slightly silty, very fine sand to sandy, silty clay. Pebbles are rarely present in the fracture below the base of the uppermost gravel layer (fig. 6, 3.4-m depth). Fracture fill usually contains more clay than the surrounding material. Horizontal or concave-upward laminae are present locally in fracture fill and probably represent individual depositional events during which sediment was washed into the fracture by storm runoff. Layers of clay on the walls of the fractures and internal clay laminae (≤ 1 mm thick) within the fill indicate multiple episodes of deposition and fracturing of the fill material. The internal clay laminae are subparallel to the fracture walls, although they branch and join on a scale of a few centimeters (fig. 7c). These internal laminae probably mark events when the fill material cracked, possibly owing to desiccation of the fill or to further tensional opening of the original fracture, which pulled the fracture fill apart. Apparently after the fill fractured, clay was deposited on the walls of the new (internal) openings, perhaps by settling out of downward-percolating water or by adhering to the walls as water seeped laterally out of the fracture and into the surrounding sediments. Similar features in fracture fill have been described by Bull (1972) and by Guacci (1979). They attributed development of these layered fracture fillings to repeated deposition of sediment carried down into the fractures by water.

Fractures below the fissures conduct water more easily than surrounding sediments, as indicated by carbonate cement and clay lining the fractures, live woody roots in the fractures, and results of a ponding test conducted in trench 3 (Scanlon and others, 1990). Carbonate cement less than 0.5 mm thick lines the walls of the fracture in the petrocalcic horizon at a 4.3-m depth at fissure 1. In addition, at a depth of 5.7 to 6.2 m, gravel is weakly cemented by calcite in a 7-cm-wide zone around the fracture (fig. 6). The fractures are preferred pathways for roots through all strata, including the gravel layers. Live roots are present in fractures as deep as 6.2 m below the ground surface. The ponding test is discussed in detail in the "Ponding test" section (p. 21–24).

Other fractures near the fissure that have reached the surface are likely to be pathways for downward-moving water. Fractures near fissure 1 are wider and are lined with gray clay or carbonate cement more commonly than are fractures farther from the fissure. Although many fractures (lined and unlined, filled and hairline) can be traced upward from polygonal fractures in the petrocalcic horizon (fig. 8), those more than about 3 m from the fissure and those beyond the ends of the fissure in trenches 2 and 5 (fig. 4) are not as wide as those nearer the fissure, which are more than 1 cm wide.

Clay-lined cavities to a depth of 2.8 m are locally present in the fracture below fissure 1. These openings probably fill periodically with water that enters the fissure at the surface. The horizontal dimensions of cavities exposed in trench walls range from 0.4 to 60 cm, but most are less than 10 cm across. Vertical extent of openings along the fracture below fissure 1 is about 5 percent of the total exposed depth of the fracture in the southeast wall of trench 3 (fig. 6). Some cavities at a depth of 2.8 m contain spiderwebs, indicating that they are connected to the ground surface through openings along or near the fissure. Some of the larger openings may be produced by or enlarged by animals burrowing near or along the fracture. Evidence of this includes rodent fecal pellets in fissure fill near the ground surface and filled animal burrows in silty sand near the fissure as deep as 2 m below the surface (fig. 9). The burrows may have been dug by badgers (*Taxidea taxus*). Badgers, which have burrowed as deeply as 2.3 m elsewhere in the western United States (Long and Killingley, 1983), have been seen

in the study area (Alan R. Dutton, Bureau of Economic Geology, personal communication, 1990).

The cavities within the fracture fillings may form as material collapsing from the overlying fissure is dispersed into the matrix of the less cemented, clast-supported gravel (fig. 6, 2.7- to 3.4-m depth), leaving open spaces in the fracture where it passes through the gravel. In the fracture at fissure 1, no cavities larger than 1 by 3 cm are deeper than 3.4 m, which corresponds to the base of the uppermost gravel layer as observed in trench 3 (fig. 6). Only a few small openings in fracture fill (mostly <0.5 cm wide) have been seen below the base of that gravel layer.

The relationship between the fissure and underlying fracture is not as apparent in trench 4, which was excavated between surface-collapse features (fig. 4). From this exposure it appears that small cavities can form along the fractures even where there is no fissure directly above. The fractures here extend upward from a 3-m depth to the base of the surface soil (30-cm depth) at about 0+06 SW and 0+12 SW (fig. 9), parallel to and flanking the interpolated trend of the fissure. These are termed fissure-bounding fractures because they lie on either side of the fissure, not below it. They are the only fractures in trench 4 in which cavities larger than about 1 by 4 cm have developed or have remained open in unconsolidated sediments above the petrocalcic horizon (figs. 8 and 9). These fractures are mostly less than 1 cm wide and narrow downward to a hairline crack lined with clay. One of the fissure-bounding fractures in trench 4 branches downward and narrows abruptly at a depth of 2.3 m (fig. 9, 0+12 SW) to a 0.2-cm-wide filled fracture lined with gray clay, similar to the fracture at a 5.8-m depth in trench 3 (fig. 6).

Numerous small, closed fractures between the fissure-bounding fractures in trench 4 are present in the crossbedded sandy unit above the massive gravelly sand (figs. 8 and 9; 1.5-m depth). They are more common here than farther from the trend of the fissure. Unlike the fissure-bounding fractures, these fractures branch upward. They are hairline fractures that are barely traceable, and all appear to be confined to this sedimentary unit.

Rubble zones in the crossbedded sand layer (fig. 9) are either caved-in burrows or fillings within collapse zones that connect along a tortuous path to collapse features at the surface. These rubble zones are bounded by fractures and may be precursors to fissures. A few fractures extend from

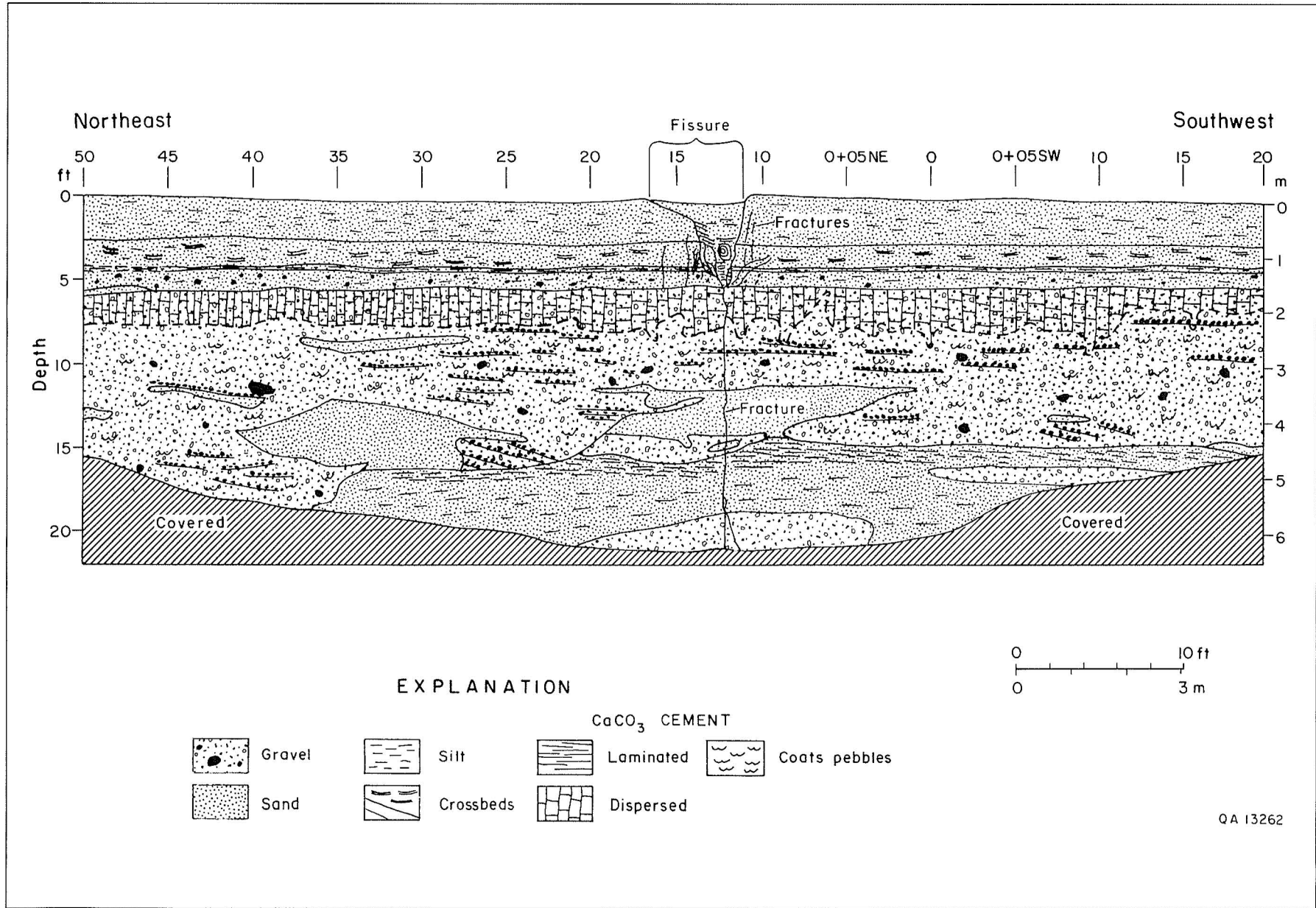


FIGURE 5. General view of southeast wall of trench 3 at fissure 1. The arbitrary horizontal coordinate system for trench logging, marked in 5-ft (1.5-m) intervals, is shown at top of figure. See figure 4 for location of trench.

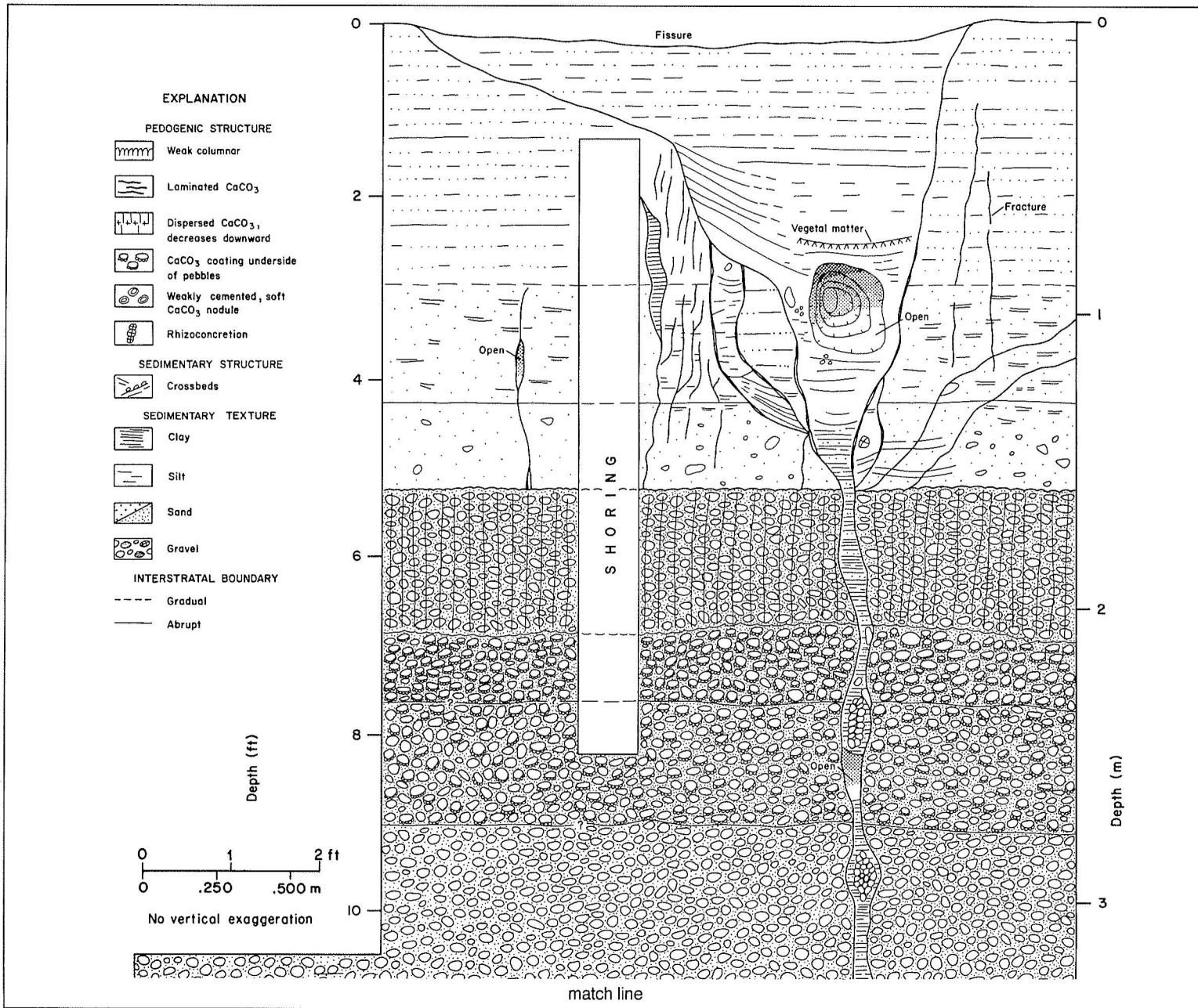


FIGURE 6. Detail of fissure 1 in southeast wall of trench.

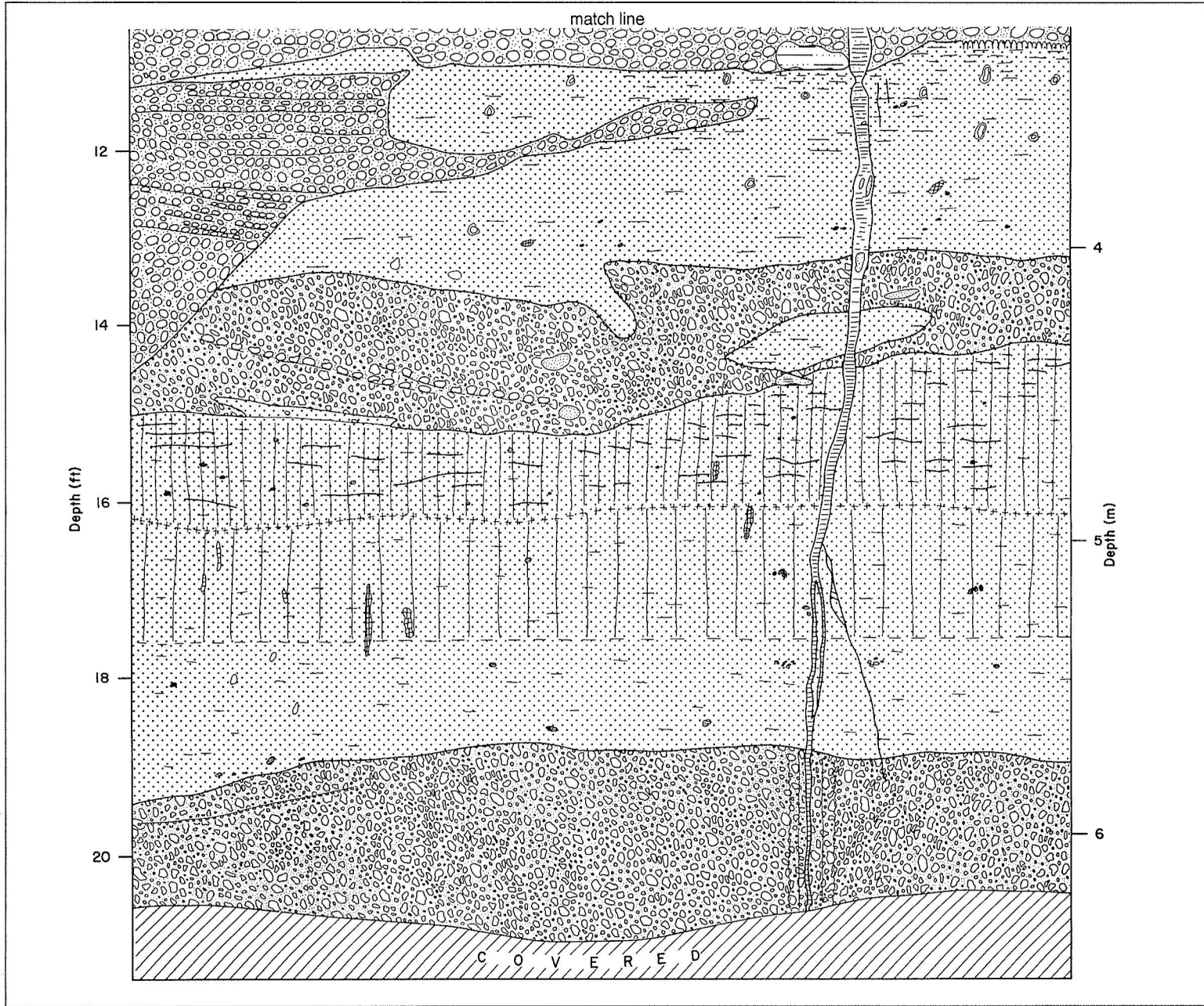


FIGURE 6 (continued)

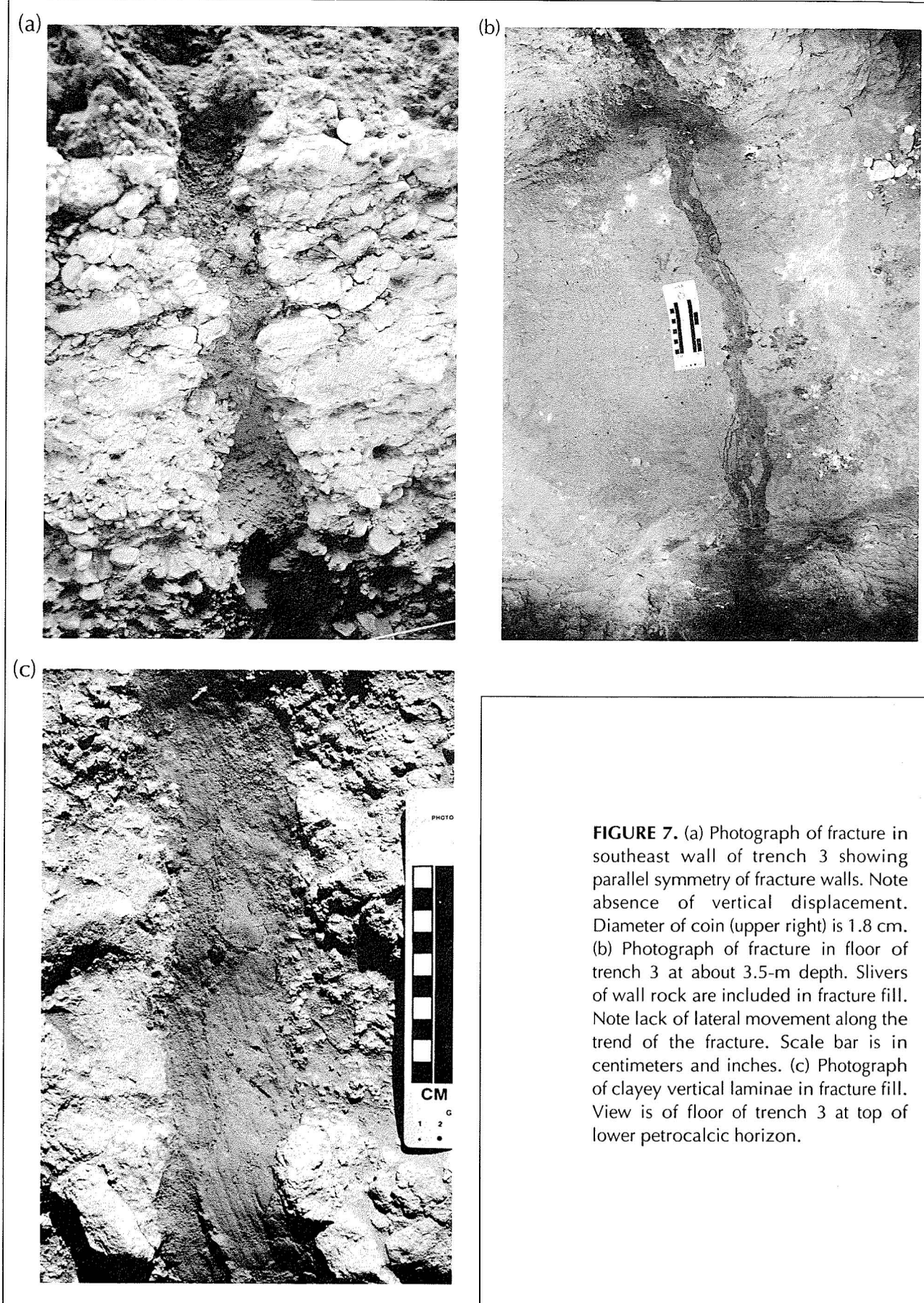


FIGURE 7. (a) Photograph of fracture in southeast wall of trench 3 showing parallel symmetry of fracture walls. Note absence of vertical displacement. Diameter of coin (upper right) is 1.8 cm. (b) Photograph of fracture in floor of trench 3 at about 3.5-m depth. Slivers of wall rock are included in fracture fill. Note lack of lateral movement along the trend of the fracture. Scale bar is in centimeters and inches. (c) Photograph of clayey vertical laminae in fracture fill. View is of floor of trench 3 at top of lower petrocalcic horizon.

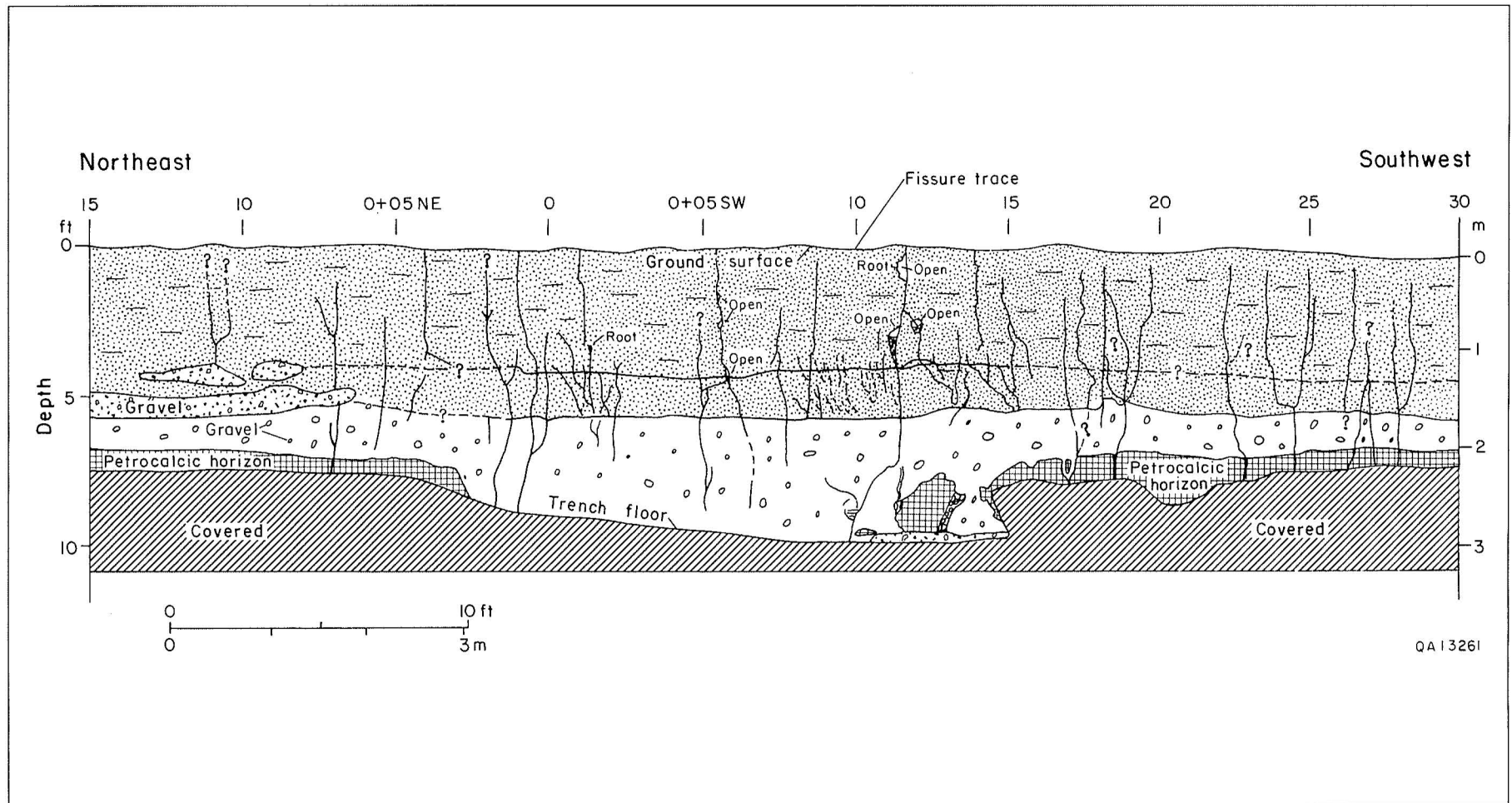


FIGURE 8. General view of southeast wall of trench 4 at fissure 1. Detailed sedimentary data are omitted to emphasize fractures. Although the fissure is not visible here, its interpolated position between adjacent collapse features (to the northwest and southeast) is shown. See figure 4 for location of trench and figure 9 for sedimentologic detail.

rubble zones upward into the overlying massive unit to within 60 cm of the surface. As with the fractures in trench 3, there is no offset across these fractures. The rubble zones consist of structureless sediment that is more silty than the adjacent crossbedded silty, fine to medium sand. Although they appear to terminate abruptly in the vertical wall of the trench, they probably continue up and down at some angle to the trench wall.

Polygonal Fractures in the Petrocalcic Horizon

Vertical polygonal fractures are ubiquitous in the petrocalcic horizon. At the study area they are present hundreds of meters from the fissures, in outcrops of the petrocalcic horizon in unpaved roads and along the channel floor of an ephemeral stream. Most of these fractures are less than 7 mm wide and are lined with carbonate that is commonly less than 1 mm thick. They outline polygons in the petrocalcic horizon that are about 1 m across. Some that are perpendicular to local slope in ditches along the county road and in the stream channel floor are wider, presumably enlarged by erosion. All fractures more than 2 mm wide in the petrocalcic horizon in trench 4 are at least partly coated with carbonate. Fractures up to 8 cm wide in the petrocalcic horizon (trench 4) are lined with carbonate up to 7 mm thick.

These polygonal fractures predate the surface fissure by several thousand years. The age of the fissure is inferred from aerial photographs. Although the fissure is not visible on photographs taken in 1971, it can be seen on those taken in 1985. The estimate of the age of the fractures is based on the presence of carbonate lining on fracture walls, which takes several thousand years to form in this region (Machette, 1985). These fractures formed independently of the fissure. Such fractures are commonly observed in well-developed calcic horizons (Reeves, 1976; Gile and others, 1981; Machette, 1985).

Fractures in the walls of trench 4 near the fissure extend upward from polygonal cracks in the petrocalcic horizon into overlying sediments, commonly to the base of the loose surface soil (fig. 8; 0+18 to 0+28 SW). This suggests that movement of the fracture-bounded polygonal blocks in the petrocalcic horizon produces fractures in the overlying sedi-

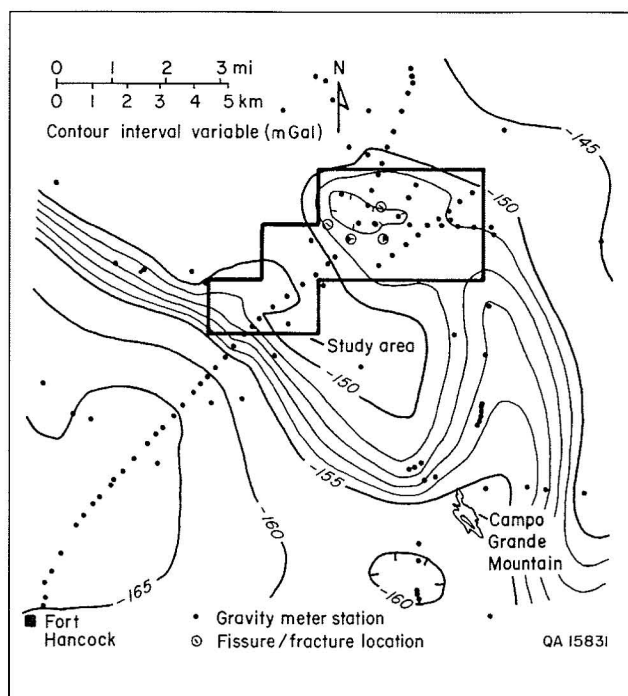
ments, perhaps as a result of desiccation of underlying sediments. Some fractures branch upward at the top of the massive, gravelly sand (fig. 8, 1.7-m depth). It appears that volume changes in the near-surface sediments allow fractures to branch upward from the rigid blocks in the petrocalcic horizon. Hairline fractures are usually open and unlined above the carbonate horizon, indicating either that they have not been preferred pathways for water movement or that they formed during excavation of the trenches. However, a root growing in one of these fractures (fig. 9; 0+1.5 SW; 1-m depth) indicates that it predates trenching.

Most of the polygonal fractures beyond the ends of fissure 1 (fig. 4, trenches 2 and 5) do not extend above the petrocalcic horizon. A few hairline fractures can be traced upward to the base of the surface soil (30-cm depth); none of these are clay lined, and they probably formed as a result of trenching. Maximum width of fractures in the carbonate horizon here is 2.0 cm, narrower than fractures near the fissure trace in trench 4.

Subsurface Geologic Structure

Structure of Cretaceous bedrock beneath the study area is not completely known. Although there are no seismic data for the area directly below the fissures, two seismic reflection surveys were run across the study area near the fissures. On the basis of the first survey, Phillips and others (1986) inferred a high-angle normal fault extending upward from Cretaceous bedrock into the Camp Rice Formation about 350 m south of and oblique to fissure 1. The interpretation of the second survey, from higher resolution data, did not show a fault in the bolson fill but did show a possible thrust ramp in the underlying Cretaceous bedrock (Baker and Keller, 1990). Several reflector discontinuities suggest that small-scale normal faults may be present in lower Pliocene deposits that overlie this zone, but they do not extend above the Fort Hancock Formation (Baker and Keller, 1990). Neither survey interpretation showed faults extending to the surface.

Gravity data show a small, shallow closed basin in Cretaceous bedrock beneath the study area (fig. 10) (Keller, 1990). Raney and Collins (1990) showed a similar, although larger, bedrock low beneath the study area on their cross section of the



Hueco Bolson (fig. 1b). The three fissures and the relict fracture in the study area are located around the margins of the small closed basin. However, no fissures have been seen along the trend of the Campo Grande fault southwest of the study area (fig. 10), where bedrock relief is much greater and where differential compaction would probably be more pronounced. The apparent absence of fissures may be due, in part, to thicker and more extensive deposits of windblown sand in the southern part of the study area, which may have obscured fissures.

FIGURE 10. Bouguer gravity anomaly map of the Hueco Bolson study area. The inferred bedrock surface rises from southwest (-165) to northeast (-145). Note small closed basin between the fissures. The steep slope between -150 and -155 mGal northwest of Campo Grande Mountain marks trend of Campo Grande fault. After Keller (1990, his fig. 7).

Detailed Investigations in the Vicinity of Fissure 1

Quaternary Stratigraphy

Interbedded sand and gravel compose the near-surface sediments in the vicinity of fissure 1 (figs. 6, 8, and 9). In these sand and gravel deposits two petrocalcic horizons are preserved—one between a depth of 1.5 and 2.7 m and the other between a depth of 4.3 and 5.4 m, as seen in trench 3 (fig. 6). The carbonate-cemented horizons formed nearer the ground surface than their present depth of burial, probably at less than 1 m deep (McFadden and Tinsley, 1985); they were subsequently covered as more sediment was deposited on the surface above them. These horizons show calcium carbonate morphology characteristic of Stages III and IV in the Machette (1985) classification of calcic soils and pedogenic calcretes. In both horizons, calcium carbonate is dispersed in the sandy matrix (Stage III) and increases concentration upward. Where the upper surfaces of the petrocalcic horizons are sandy, the carbonate cement is laminated and the fracture

surfaces are locally laminated (Stage IV). Development of these textures in the desert Southwest takes at least 25,000 yr (Gile and others, 1981). All of the other near-surface strata in the vicinity of fissure 1 are weakly cemented and friable yet competent enough to fracture (figs. 5 and 6).

Near-surface strata (<6-m depth) apparently did not control development or location of fissure 1. The projection of fissure 1 in trench 4 (fig. 8, 0+02 NE to 0+12 SW) overlies a 4-m-wide gap in the upper petrocalcic horizon. Similar irregular gaps also are present in the petrocalcic horizon near the relict fracture. In contrast, neither a fissure nor a fracture is present at the northeast end of trench 4 and in trench 5, even though the petrocalcic horizon has been completely eroded locally and is overlain by gravel deposits. The opposite situation exists at trench 3, where the fissure overlies an uneroded calcic horizon composed largely of carbonate-cemented gravel, which extends well beyond both sides of the fissure (fig. 5).

Hydrology

Moisture flux

The hydrologic study at fissure 1 was undertaken to determine whether downward moisture fluxes are higher along surface fissures than at other geomorphic settings. Hydraulic and chemical parameters were measured to evaluate moisture flux in the fissure, fracture fill, and surrounding sediments. Soil samples collected from three boreholes (68, 69, and 70) in the vicinity of fissure 1 (fig. 4) were analyzed in the laboratory for grain-size distribution, gravimetric moisture content, water potential, and chloride concentration. Water potential data are used to evaluate the direction of water movement because liquid water flows from regions of high to low water potential. Chloride concentrations in soil samples provide a qualitative estimate of the moisture flux through the unsaturated zone because chloride concentrations are inversely proportional to moisture flux. Low chloride concentrations indicate high moisture flux because chloride is leached, and high chloride concentrations indicate low moisture flux because chloride is concentrated by evapotranspiration. In addition to laboratory measurement of various parameters, moisture content was monitored in the field in three neutron-probe access tubes (65f, 66f, and 67f) drilled adjacent to the other three boreholes (fig. 4) to evaluate downward movement of recharge pulses. One access tube (65f) was installed in the fissure; the other two access tubes were placed at distances of 3 and 6 m along a line perpendicular to the general trend of the fissure. Moisture content was logged monthly at 0.1-m intervals from a depth of 0.3 to 6 m. These procedures are described in detail in Scanlon and others (1991).

Soil texture beneath the fissure is similar to that in the adjacent area (fig. 11a, f, and k). There is no systematic relationship between moisture content of the sample and its proximity to the fissure. Gravimetric moisture content ranged from 0.03 to 0.11 g g⁻¹ in soil samples from boreholes 68, 69, and 70 (fig. 11b, g, and l). Variations in moisture content in boreholes 68 and 69 (high in clay-rich material and low in gravelly zones) were related to soil texture. This relationship between moisture content and texture was not as well defined in soil samples collected from borehole 70. Monthly mon-

itoring of moisture content in access tubes 65f, 66f, and 67f from October 1989 through February 1990 indicated no temporal variations in moisture content below 0.3 m (fig. 12a, b, and c). During the same period about 1.5 cm of rain fell at the study area. Temporally invariant moisture content is inconclusive evidence of the absence of downward water percolation because the accuracy of logging moisture content with a neutron probe (accurate to 0.01 m³ m⁻³) may be insufficient to detect low moisture fluxes that could occur.

Water potentials decreased down to a 0.4- to 0.7-m depth and then increased to a total depth of 8 to 9 m in boreholes 68, 69, and 70 (fig. 11c, h, and m). The decrease in water potential near the surface indicates a potential for downward liquid water movement and reflects infiltration of a recent precipitation event. The increase in water potential below this shallow zone represents a driving force for upward liquid water movement. The highest water potentials (-0.2 to -0.4 MPa) in soil samples from the base of these boreholes are higher than those (~-2 MPa) from the same depth intervals in boreholes drilled in ephemeral stream and interstream settings and suggest that soils near the fissures are wetter than those in other geomorphic settings.

The chloride profile at the fissure is characterized by low concentrations (<100 g Cl m⁻³ soil water), similar to those of chloride profiles in adjacent boreholes 69 and 70 (fig. 11d, i, and n), suggesting that the fissure affects flow from an area wider than 6 m. There is no systematic variation of chloride concentration with depth. The low chloride concentrations indicate that chloride is being flushed downward in the region of the fissures. Low chloride content, characteristic of the area of the fissures, differs markedly from chloride profiles measured in ephemeral stream and interstream settings, which have maximum chloride concentrations of 2,000 to 9,000 g m⁻³ at depths of 1.3 to 4.6 m. These data suggest that moisture fluxes near the fissures are much higher than those in other sampled ephemeral stream and interstream areas.

Ponding test

A ponding test was conducted in trench 3 at fissure 1 (fig. 4) to evaluate flow in the fissure relative to that in surrounding sediments. The 4-m² ponded area was excavated to a depth of approximately

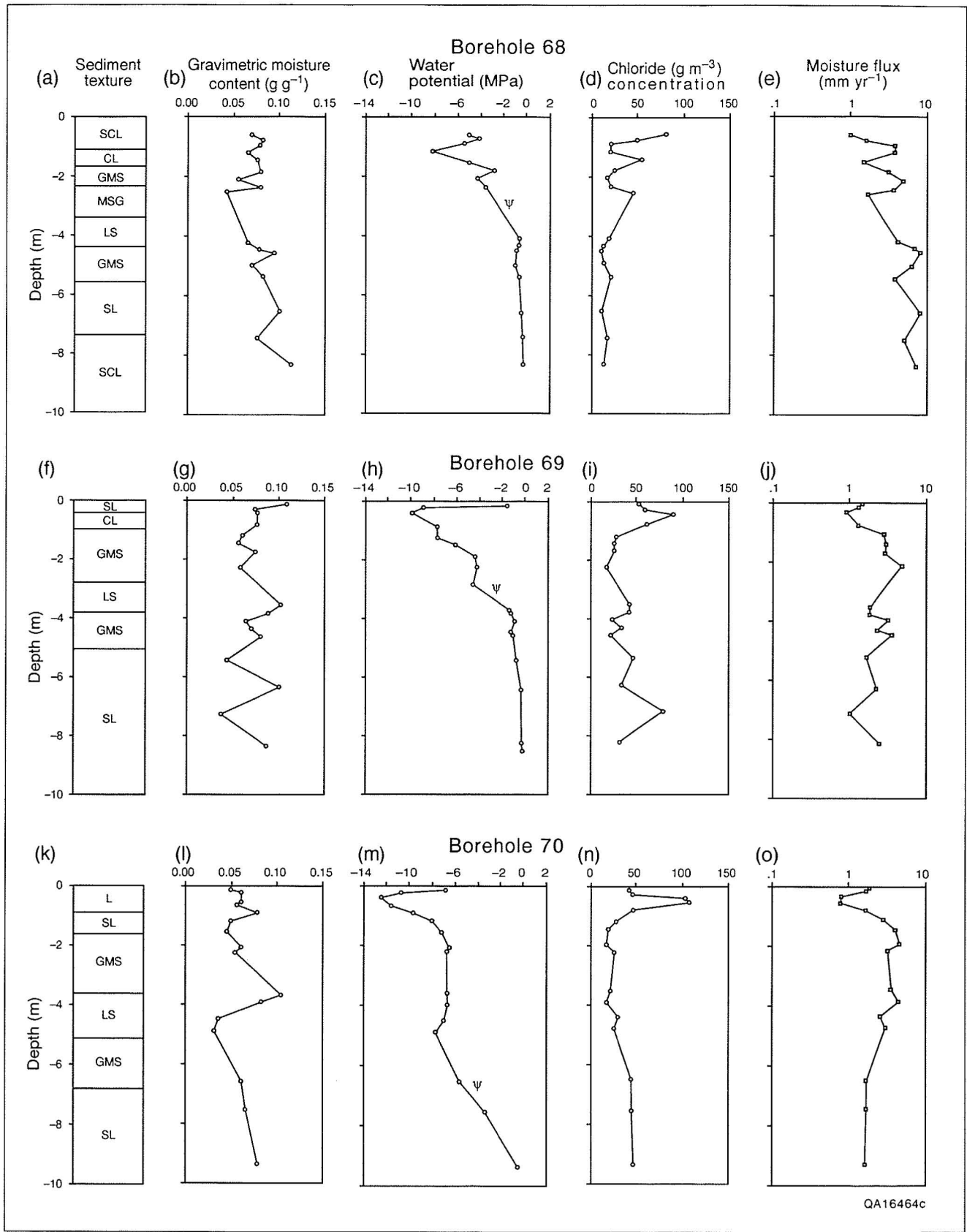


FIGURE 11. Profiles of sediment texture, gravimetric moisture content, water potential, chloride concentration, and moisture flux for boreholes 68, 69, and 70. Sediment texture abbreviations are derived from sediment categories presented in figure 14. See figure 4 for locations of boreholes.

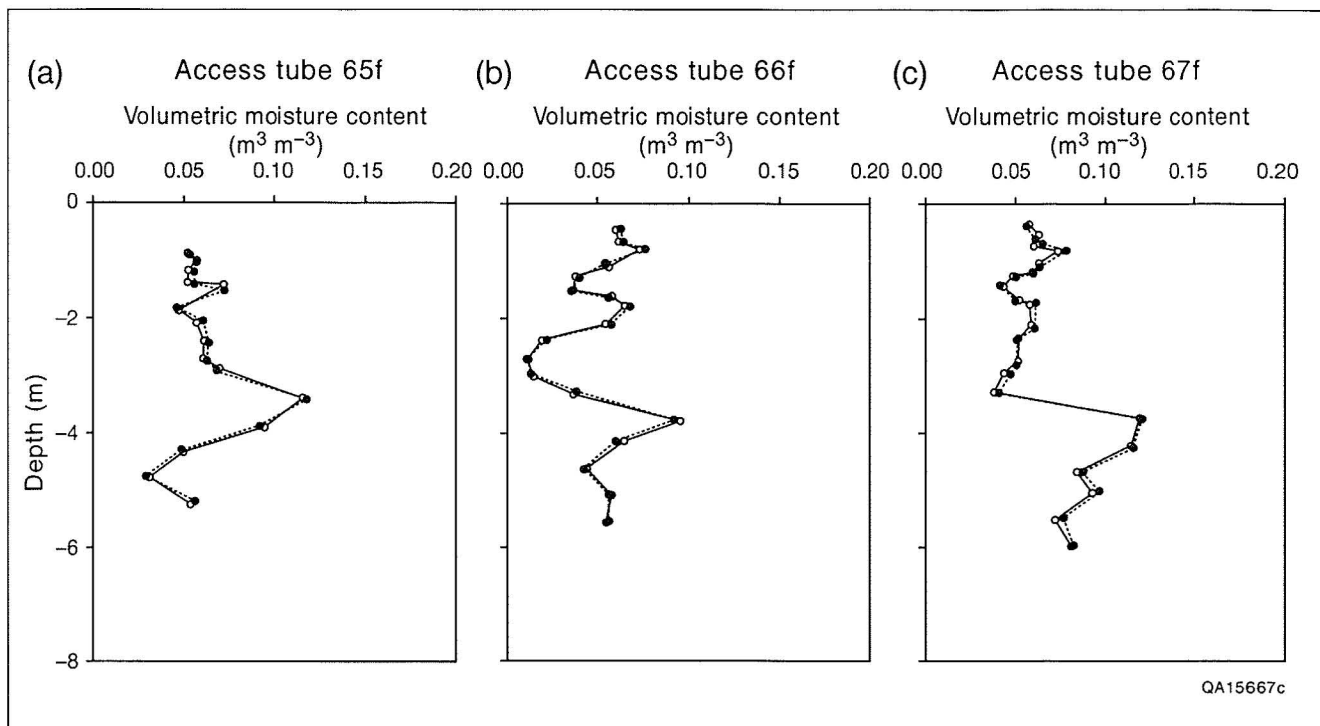


FIGURE 12. Variation in volumetric moisture content with depth and time in (a) access tube 65f, (b) access tube 66f, and (c) access tube 67f. Water content was monitored monthly in each access tube from October 1989 through February 1990. Volumetric moisture content was measured from 0.3-m depth to the bottom of each tube in depth increments of 0.1 m. See figure 4 for location of access tubes.

4 m and was covered with water to a depth of 0.4 m for approximately 6 hr. Because it is chemically conservative and background concentrations in interstitial water are zero, bromide was added to the water as a tracer at a concentration of 330 g m^{-3} . Water for the ponding test was obtained from a local well and had a naturally high chloride concentration (240 g m^{-3}). The walls of the ponded area consisted of natural sediment, and lateral flow of water from the pond was allowed. The ponding site was not instrumented with neutron-probe access tubes or soil solution samplers so that artificial pathways for the ponded solution would not be created. After 6 hr of ponding, the ponded area was excavated with a bulldozer to a depth of 2.2 m below the ponded surface. Soil samples were collected at depth intervals of 0.2 to 0.4 m in the fracture fill and along a profile perpendicular to the fracture at depths of 0.2, 0.5, 1.0, 1.5, and 2 m below the ponded surface (fig. 13). These soil samples were analyzed for grain-size distribution

and moisture content. Soil-water extracts from these samples were analyzed for chloride concentration by titration and for bromide concentration by ion chromatography.

Soil texture in the fracture fill is similar to that in nearby sediments (fig. 14a). Gravimetric moisture content after the ponding test was generally high throughout the sampled zone of the fracture fill and ranged from 0.16 to 0.29 g g^{-1} (fig. 14b). A zone of low moisture content (0.04 to 0.06 g g^{-1}) at a depth of 0.7 to 0.9 m corresponded to a gravel-rich layer. Excavation to 2.2 m below the ponding surface was not deep enough to reach the base of the wetting front in the fracture fill; however, the wetting front only penetrated approximately 1.4 m in the adjacent material.

Soil-water bromide concentrations were high in the fracture fill to a depth of 2.2 m, whereas bromide concentrations were close to background values (zero) at a depth of 1.4 m in adjacent sediments (fig. 14c). Although the ponded area extended 1 m

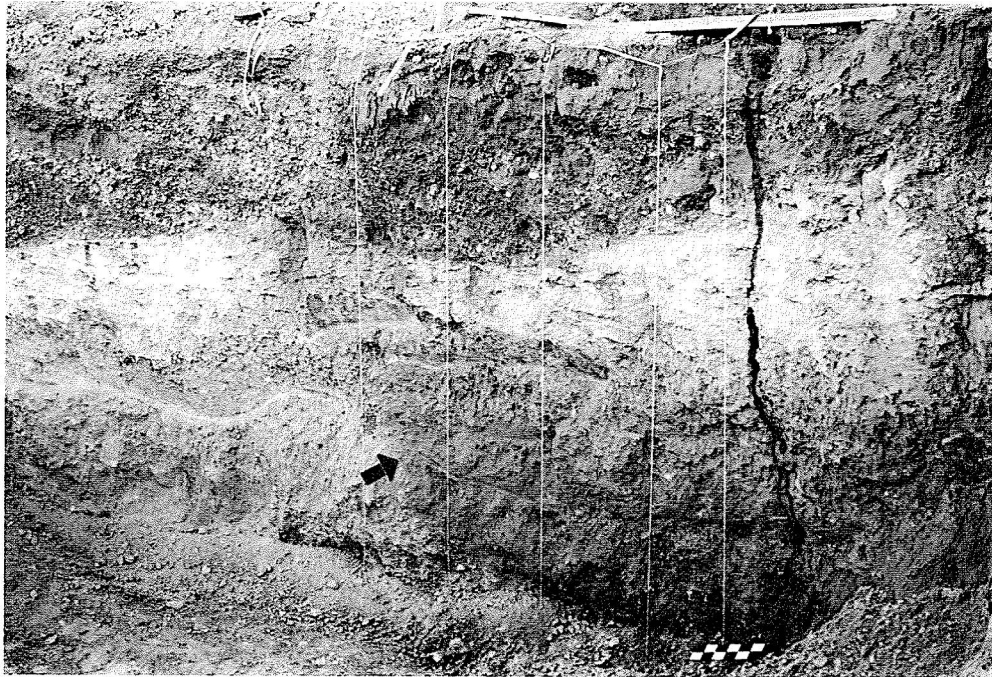


FIGURE 13. Photograph of southeast wall of trench 3 after further excavation below level of ponding test (top of photograph). Ponding test was conducted before trench was deepened. Hanging strings mark approximate locations of sampling profiles for cross sections in figure 14. Edge of wetting front (arrow) is visible as dark zone convex toward the left.

from the fracture, high bromide concentrations were measured in soil-water samples collected 1.5 m from the fracture. No bromide was detected in the profile 2 m from the fracture fill. Bromide data indicate that the lateral movement of the infiltrated water in the coarse-grained material 0.7 to 0.9 m below the pond was less than in finer grained material above and below. The distribution of chloride was similar to bromide, except that background chloride concentrations were not initially zero (fig. 14d). The water content and solute data suggest preferential flow of water in the fracture fill relative to the surrounding sediments.

It is difficult to compare the results of the ponding test with moisture content, water potential, and chloride data obtained from the boreholes because of the differences in spatial and temporal scales examined. The ponding test was a short-term tracer experiment that included detailed sampling of the fracture fill and adjacent sediments. The data from boreholes represent a much longer

period. Although neutron-probe access tubes were installed and boreholes were drilled into the fissure, it is doubtful that the soil samples collected from borehole 68 contain only fracture fill; as a result, data from borehole 68 do not represent fracture fill alone. Even though the chloride data represent a longer period (up to 400 yr) than that considered in the ponding test, they showed higher moisture fluxes near the fissures than at other geomorphic settings, which is consistent with the ponding-test results. The low chloride concentrations measured in soil samples from all three boreholes drilled along a line perpendicular to the fissure suggest that the zone of high moisture flux extends horizontally several meters from the surface fissure. Thus, the fissures and fracture below it are preferential pathways for water movement in the shallow (<6 m) subsurface. The fissures concentrate runoff, and the fractures provide avenues for rapid moisture and solute movement.

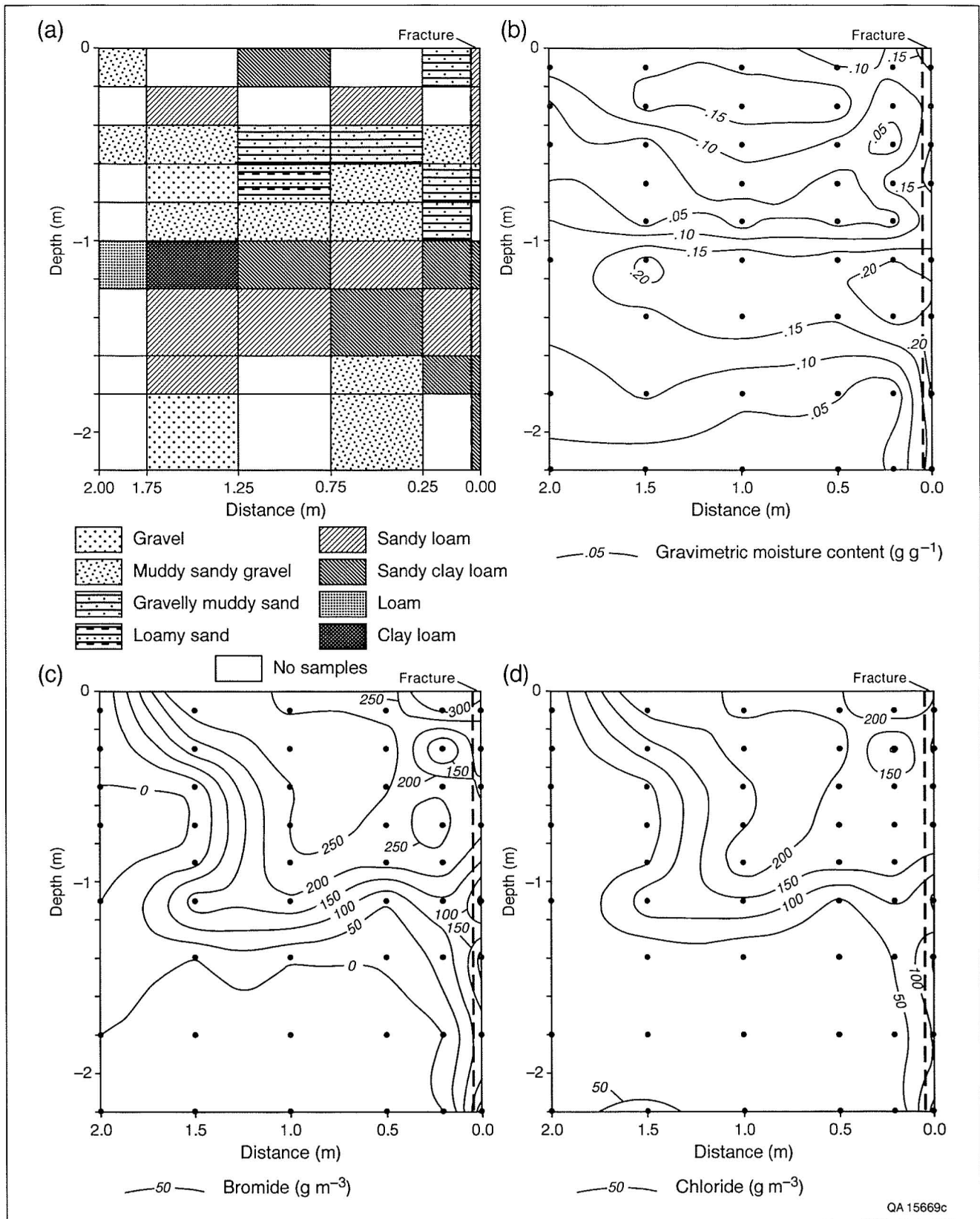


FIGURE 14. Schematic cross sections constructed from analyses of soil samples collected beneath ponding surface in trench 3: (a) sediment texture, (b) gravimetric moisture content, (c) bromide concentration, and (d) chloride concentration. Top of figures is bottom of pond at 4-m depth in trench 3. See figure 4 for location of ponded site.

Other Fissures in the Region

Green River Valley

Several investigators have reported surface fissures in the Trans-Pecos region of Texas and in north-eastern Chihuahua, Mexico (fig. 15). In an early account, Baker (1927, p. 40) described "deep, straight, and narrow cracks . . . [cutting] . . . the clays of the arroyo beds and the gravels of the benches" in the Green River valley. This site is about 100 km southeast of the study area (fig. 15; table 2). Baker attributed the fissures to earthquake-related failure and speculated that they may have formed in 1887 during the "great earthquake in northeastern Sonora," more than 320 km away. However, he provided no evidence for either the origin or the age of the fissures. Underwood and DeFord (1975) reported that no fissures were visible in this area on aerial photographs taken in 1950, implying that Baker's fissures had filled in. But they recorded the appearance of a 740-m-long fissure that formed in the valley in May 1959 (Underwood and DeFord, 1975), cutting across a road. However, an extensive network of polygonal and branching fissures is present on photographs taken in 1957 and in 1980. These fissures, unlike those described by Underwood and DeFord (1975), do not cross roads. Because descriptions of the Green River valley fissures by Baker (1927) and Underwood and DeFord (1975) lack the detail necessary to locate the fissures accurately, it is unknown whether the fissures they reported are the same as those on the photographs. The network of fissures visible on photographs taken in 1980 is 2,700 m long, about 400 m longer than the fissures visible on the 1957 photographs. The long dimension of the network is subparallel to the valley axis.

Pumping of ground water probably did not affect fissure development in the Green River valley. Of the 11 wells in the valley within an 8-km radius of the fissures, none are used for irrigation, and only 2 are known to have been drilled before 1927 (White and others, 1980).

Quitman Canyon

Albritton and Smith (1965) reported "earthquake cracks" in alluvium near the center of Quitman Canyon, about 60 km southeast of the study area

(fig. 15). According to Albritton and Smith, the cracks were "said to have formed" during the Valentine, Texas, earthquake (August 16, 1931), whose epicenter was 105 km east of Quitman Canyon (Sellards, 1932). However, they offered no evidence to support this statement, which is contradicted by an eyewitness, R. H. Espy, a resident of Eagle Flat (fig. 15). Underwood and DeFord (1975) reported that Espy saw the fissures in Quitman Canyon during a cattle roundup in about 1924, 7 yr before the Valentine earthquake. Furthermore, Sellards (1932) compiled observations from localities throughout the region where the earthquake was felt, including Sierra Blanca and Van Horn (fig. 15), and found that no disturbance of the ground was detected after the 1931 earthquake except in the town of Valentine. The apparent absence of surface cracks from the 1931 earthquake suggests that the earthquake origin attributed for the fissure described by Albritton and Smith (1965) is incorrect. Although the lack of reported "earthquake cracks" in the region around Valentine may have been due to a dearth of observers, it is more reasonable to accept Espy's personal account that the cracks in Quitman Canyon existed before the 1931 earthquake than to accept an unsupported claim of an earthquake-related origin.

The Quitman Canyon fissures, which are still visible, lie at the toe of a dissected alluvial fan, cutting Quaternary alluvium at the surface. Two sets of collapse features roughly perpendicular to one another intersect to form polygons up to 390 m wide (on the 1957 aerial photographs). One set of fissures trends N10°–25°W, parallel to topographic contours, to faults in the Quitman Mountains (about 6 km to the west-northwest), and to the valley axis; these fissures were as long as 4.2 km on aerial photographs taken in December 1957 (table 2). The other set consists of shorter fissures that trend N65°–80°E. A calcic soil horizon composed of carbonate-cemented sand is locally present at the surface; it is exposed in the fissure walls at depths of less than 1 m. The major northwest-trending collapse features are perpendicular to the ephemeral stream channels between fan remnants and intercept runoff. Woody vegetation (mostly mesquite [*Prosopis glandulosa*] and tarbush [*Flourensia cernua*]) is more abundant within a few meters of the fissures than farther away. These plants are especially sparse downslope from

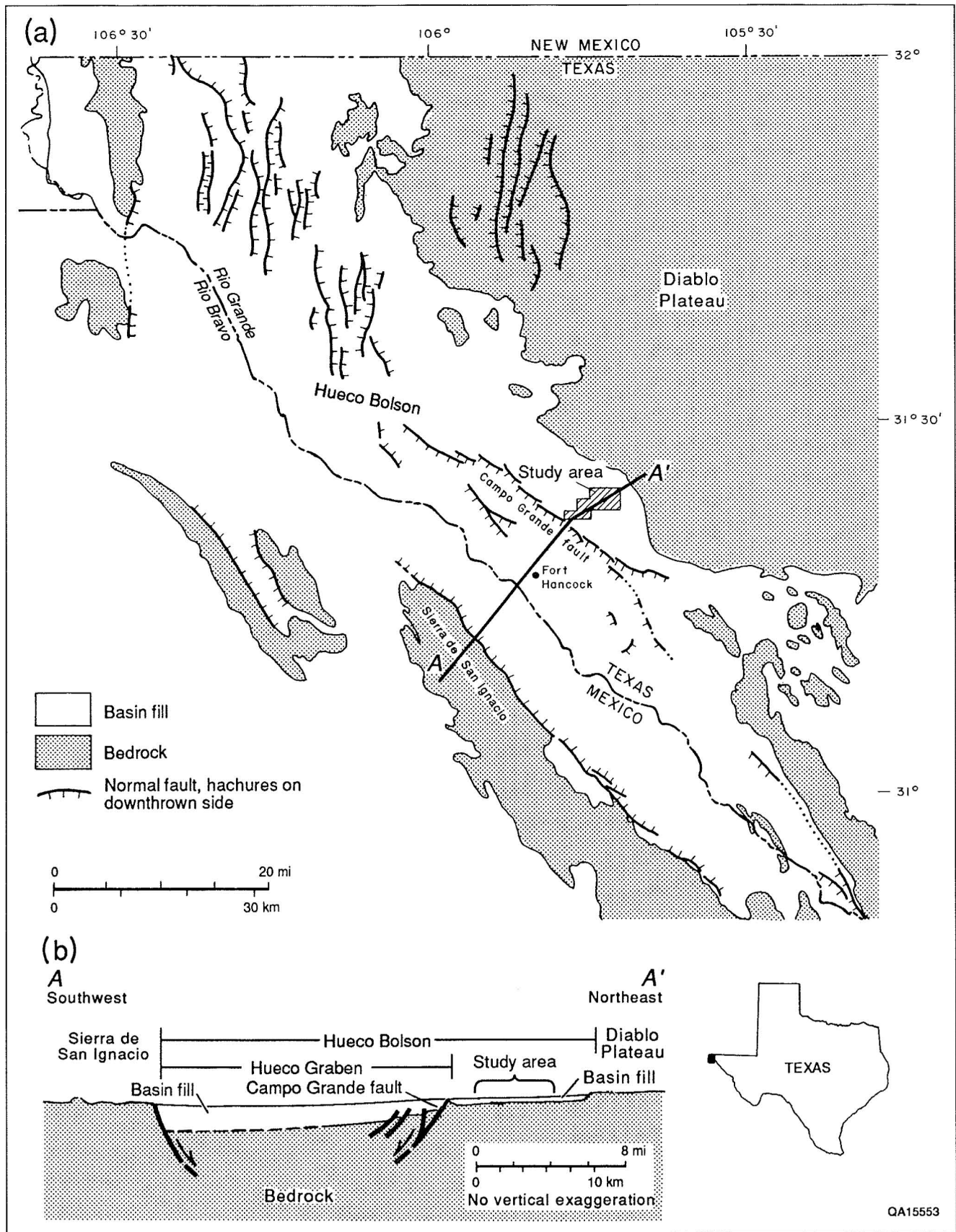


FIGURE 15. Map of fissures in region of the study area that have been reported in the literature or observed in the field. The boundary between basins and bedrock outcrops (stippled) is generalized from Dirección General de Geografía (1981, 1982) and Henry and others (1985).

the fissures. The lack of vegetation suggests that the fissures capture all but the largest overland flows and reduce moisture available for vegetation downslope.

In 1989 the fissures in Quitman Canyon locally showed evidence of recent collapse. Fissure walls were steep and unvegetated. One segment was 3.55 m deep but only 75 cm wide—deeper than any fissure at the study area in the Hueco Bolson. The width/depth ratio for this segment is very low (0.2) (table 2), indicating that it is relatively young, has an unstable profile, and is still undergoing collapse. Other segments of the Quitman Canyon fissures have filled with sediment washed in from upslope and now have width/depth ratios as high as 5.

The width/depth ratio of fissures provides a means of assigning relative stability of fissures. Width/depth ratios range from 0.1 to 28, but most of the values fall below 5 (table 2). These ratios indicate that fissure segments having width/depth ratios less than about 5 are probably still undergoing collapse, whereas those having ratios greater than about 5 are filling and widening.

Another set of polygonal fissures, about 4 km south of those previously described, was observed on 1957 aerial photographs of Quitman Canyon. The longest fissure was about 200 m long in 1957, similar to the length of fissure 1 in the Hueco Bolson study area.

A third set of fissures in Quitman Canyon was discovered in September 1985. In 1989 these fissures were reported to form a rectilinear pattern (Sergent, Hauskins and Beckwith, 1989). Individual fissures were up to about 300 m long, 1.8 m wide, and 1.5 m deep.

Water pumping in Quitman Canyon did not affect fissure development there. None of the wells reported by White and others (1980) were drilled before 1940. Fewer than 20 wells lie within an 8-km radius of these fissures; none are used for irrigation. Water level in one well dropped 0.8 m between 1966 and 1972. The small amount of water produced from these wells at depths of 88 to 137 m probably has no effect on the fissures today.

Bolson El Cuervo

Haenggi (1966) and Underwood and DeFord (1969) reported on fissures formed in 1959 in Bolson El Cuervo, northeastern Chihuahua (fig. 15), about 140 km south-southeast of the study area. Under-

wood and DeFord (1969) attributed formation of these fissures to drying of alluvium during a severe drought that lasted from 1950 to 1956. No details regarding their length, width, or depth are available.

Eagle Flat

Fissures have been reported at Eagle Flat, about 80 km southeast of the study area (fig. 15). According to Underwood and DeFord (1975, p. 137), the fissures were first observed in 1927 or 1928—three or four years before the 1931 Valentine earthquake. R. H. Espy, owner of the property where the fissures occurred, told them that the fissures had “appeared suddenly” in a pasture that he had ridden over a week earlier. Underwood and DeFord (1975) reported that the longest fissure was about 760 m long and that orthogonal fissures that crossed the main fissure were about 180 to 240 m long. Aerial photographs taken in 1957 and examined during this study showed that the main fissure was about 910 m long at that time. The main fissure was arcuate and convex toward the southeast and approximately perpendicular to local drainage.

By 1989 the main fissure at Eagle Flat had been widened and filled by overland flow. Locally, it was up to 17 m wide and about 60 cm deep. It had the highest width/depth ratio (up to 28) of any fissure examined during this study, indicating that it had been eroded more than the others and has a stable profile that is no longer susceptible to collapse (table 2). Earthen dams less than 2 m high have been built across the fissure, which acts as an ephemeral stream channel. The surface immediately upslope from this fissure aggraded at some time in the recent past, burying a fence with about 1 m of sediment. Another, younger fissure has developed on this aggraded surface upslope from the first fissure. The second fissure is up to 1.7 m wide and 70 cm deep and has an intermediate width/depth ratio (up to 2.7). It is nearly continuous but has a few bridged-over segments. This fissure is subparallel to the older fissure and is connected to it by small gullies that have eroded upslope from the older fissure. A third fissure, now forming upslope from the second, is only 65 m long, much shorter than either of the other two. It consists of individual collapse features up to 35 cm wide and 80 cm deep (width/depth ratio = 0.4). The length, width/depth ratio, and overall appearance of this fissure are similar to those at the Hueco Bolson study area.

Apparently the surface-collapse process is moving upslope, forming fissures subparallel to the oldest fissure. Holzer (1976) described similar zones of parallel fissures about 30 m wide wherein secondary fissures were subparallel to the main fissure and a few tens of meters long. The younger collapse features at Eagle Flat may be contributing to stabilization of the oldest fissure by capturing runoff from upslope. The oldest fissure appears to have stopped collapsing and is gradually being filled and degraded by surface processes.

Only one of four documented wells within 8 km of these fissures existed before 1927 (White and others, 1980). None are used for irrigation; two are not used at all. Clearly, water production from these wells is insufficient to cause tensional fracturing associated with fissures.

Salt (Wildhorse) Flat

Goetz (1977, 1985) described giant desiccation cracks in Salt (Wildhorse) Flat in the Salt Basin Graben, 100 km east of the study area (fig. 15). The cracks lie at the base of an alluvial fan. The longest fissure (800 m) is perpendicular to ephemeral stream channels flowing east-northeastward. This fissure is slightly arcuate, concentric to a closed basin to the east. The longest fissures in this polygonal system of cracks trend roughly north-south. Smaller, shorter fissures connect the longest fissure and others parallel to it to form polygons.

The oldest record of these fissures is on aerial photographs taken in 1946 (Goetz, 1977). The fractures may have existed for months or years before the collapse features appeared at the surface. According to Goetz (1977), the most important process contributing to the formation and growth of these cracks is desiccation of the surface and subsurface caused by prolonged drought and ground-water withdrawal by pumping. Nine stock or domestic wells are within about 8 km of the fissures in Salt Flat (White and others, 1980). The date of drilling is known for only one (1963); the others are described as "old," or they have no record of date completed. Between 1953 (when fissures had already appeared) and 1972, water levels in these wells fell between 1.11 and 7.08 m (White and others, 1980). Water level in one well declined 10.6 m between February 1962 and January 1964, then rose 9.4 m by January 1965. It is unknown if this fluctuation is representative of other

wells in the area. The amount of ground-water lowering that occurred before 1953 is unknown. Depth to water in 1972 ranged from 35.9 to 70.4 m. None of these wells were used for irrigation, and none are closer than about 1.6 km from the fissures.

Goetz (1985) also observed that the longest cracks are parallel to a series of nearby fault scarps that cut alluvium and concluded that these dominant fissures probably overlie a Holocene fault that is covered by bolson sediments at the surface. Goetz (1977, p. 89) speculated that the parallelism of the longest fissures in separate polygons may be the result of "uneven subsidence" (that is, differential compaction) across a buried fault. She proposed further that abrupt movement on this inferred fault during the 1931 Valentine earthquake may have caused failure of the alluvium, which was already undergoing brittle failure caused by desiccation at depth. However, this proposed earthquake origin is based on the similarity between these fissures and the description of the "earthquake cracks" in Quitman Canyon by Albritton and Smith (1965). As noted in a preceding discussion, the earthquake origin proposed by those authors is contradicted by an eyewitness account. The polygonal pattern of fractures at Wildhorse Flat indicates that desiccation is an important part of the mechanism by which those fissures are forming.

Ryan Flat

Fissures appeared recently south of Valentine, Texas (fig. 15), that had formed on April 21 or 22, 1990. These fissures branch complexly from a main fissure that is arcuate but trends generally north-westward. In May 1990 the main fissure was more than 500 m long. Deron Kasparian, manager of the property where the fissures formed, said that the fissure continued for about 400 m farther southeast on the adjacent property. Total length may be as much as 900 m, about six times longer than fissure 1 in the Hueco Bolson study area.

At its deepest point the main Ryan Flat fissure was 2.2 m deep and 70 cm wide. It had the lowest width/depth ratio (0.1) (table 2) of any fissure examined in this study or described in other reports on fissures. This ratio is consistent with the observation that width/depth ratio is an approximate indicator of a fissure's age. Zones of interconnected sub-parallel surface fractures along the trace of the fissure are up to 1.7 m wide. At the ends of these zones,

the surface fractures radiate away from the midline of the fracture zone.

The fissure was discovered Sunday afternoon, April 22, 1990, when a local resident was driving southward on the unpaved county road that the fissure crosses. His pickup wheels sank part way into the fissure. He had been en route to a neighboring ranch (the Nancy Anne Ranch) to help move a vehicle that was stuck in the mud produced by a heavy rainfall that had occurred the day before. About 11.2 cm of rain was recorded at the Nancy Anne Ranch 4.8 km southwest of the fissure. Approximately 7.5 cm of rain fell at the site of the fissure (Jeff Wiley, Antelope Farms, personal communication, 1990). Rainfall lasted about an hour and ended before dark on Saturday, April 21.

According to Diane Doser (Department of Geological Sciences, The University of Texas at El Paso), the record from a seismograph at McDonald Observatory near Alpine, Texas, does not show that any earthquakes occurred on April 21 or 22, 1990. Therefore, the Ryan Flat fissures did not form as a result of concurrent seismic activity.

The main Ryan Flat fissure appeared at the surface after collapse of the roof over a subsurface cavity. Roof collapse began along the midline above the cavity and proceeded outward, incorporating blocks of material that were bounded by fractures along the fissure trend (similar to the fissure-bounding fractures at trench 4 in the Hueco Bolson study area). Locally, 1.5-m³ blocks of material fell into the fissure, remaining largely intact. There is no evidence of lateral offset or downward movement of one wall of the fissure relative to the other.

Traces of an old fissure are present near the 1990 Ryan Flat fissure. Elongate, shallow swales and aligned mesquite bushes adjacent and parallel to the new fissure are evidence that the newest fissure is opening where an older fissure existed before. Unlike the fissure at Eagle Flat, the new fissure here is downslope from the older feature, indicating that the older fissure does not capture all overland flow and that some of the flow continues downslope to the younger fissure.

On the basis of field examination, near-surface sediments in which the Ryan Flat fissures formed are stronger when dry than when wet. Sediments at this location are predominantly silty, clayey sand, with downward-translocated clay concentrated in a zone about 13 cm deep. The zone of clayey sand is more competent when dry than is overlying sediment

under the same conditions. It appears to be a kind of natural adobe that forms near the surface when soil temperatures are high. This horizon may allow the roof of a cavity to resist collapse for some time, until water reduces its strength. Roy Kelley, a local resident, was riding his horse near the site of the present-day fissures in 1935 or 1936, after a heavy rain, when the horse sank to its belly into the ground. Kelley recalled that he did not see any cracks at the surface. Apparently, the weight of horse and rider exceeded the strength of the roof that bridged a near-surface soil pipe.

Observations by residents of the valley indicate that isolated collapse features are common around Valentine. Kelley has long observed small (<0.1 m²) sinkholes on his land near the south edge of Valentine. In May 1990, a 30-m-long crack trended roughly north-south in that area. The crack formed soon after about 2.5 cm of rain fell on April 21. Bo White, another local resident, said that "you can't run a horse in this country," because of the risk of stepping in one of these holes. White once found a dead bull in a collapse feature; the animal had been trapped in the hole and died. The roof of the collapse feature probably fell under the beast's weight, and it was wedged into the hole, unable to escape. The Ryan Flat fissure was the first such laterally continuous collapse feature that White had seen in the area, however. Richard Calderon, another long-time resident, said that cracks appeared southwest of the town cemetery as a result of the 1931 earthquake. Calderon, who was familiar with this piece of land because his father had farmed a few acres there at that time, said that he had not seen cracks there before the earthquake. He said that the cracks reopen every time it rains. Indeed, fresh cracks and sinkholes were observed during a visit to that locality in May 1990, just weeks after the heavy rains of April 21.

Several water wells are near the Ryan Flat fissures, but their effect, if any, on fissure formation is not straightforward. Two water wells are within 1 km of the fissures, and 23 more are located within a 9-km radius. The deepest well is 1,230 m deep; water level in these wells ranges between 62 and 125 m below land surface. Most of these wells were drilled in 1979. Maximum ground-water pumping occurred from 1979 to 1982; the pumping has decreased since that time. Water levels declined as much as 62 m from 1979 to 1982, then rose from 1982 to

1985, but not to original prepumping levels. Ten other wells in Ryan Flat were within an 8-km radius of the fissure location in 1980 (White and others, 1980). Depth to water in the 1970's ranged from 64.4 to 96.9 m. Water level actually rose in one well 0.34 m between 1955 and 1973. Records for other wells are not published. Given that the fissures are located within old, degraded swales, the original collapse probably occurred in the 1930's, long before pumping began. Furthermore, no fissures have been reported where water level has declined the most. The most recent collapse occurred several years after maximum water-level decline.

Hueco Tanks

Fissures were reported about 4 km west of Hueco Tanks National Monument, El Paso County, in August 1990 and were visited by personnel from the Department of Geological Sciences at The University of Texas at El Paso (fig. 15) (Mark Baker and Duncan Moss, The University of Texas at El Paso, personal communication, 1990). The fissures, which formed between August 11 and 14, 1990, after a heavy rainfall, were as much as 2.2 m

deep and 1.2 m wide. They crossed an unpaved road at the base of an alluvial fan, about 1.1 km south of Jarilla Tank. Where they crossed the road the fissures were 1.8 m deep and 1.1 m wide. The fissures branched to form incomplete polygonal networks. Total length of the longest fissure was about 190 m (Duncan Moss, written communication, 1990). Older fissures east of the road contained spiderwebs, indicating that they had existed for some time before the fissure appeared in the road.

These older fissures may be part of a network of fissures visible on photographs taken in 1942 and in the 1960's. The fissures shown on the photographs are adjacent to and south of the 1990 fissures. The older fissures formed incomplete polygonal networks extending roughly north-south for a maximum of 750 m. The long axis of this network is subparallel to nearby bedrock outcrops.

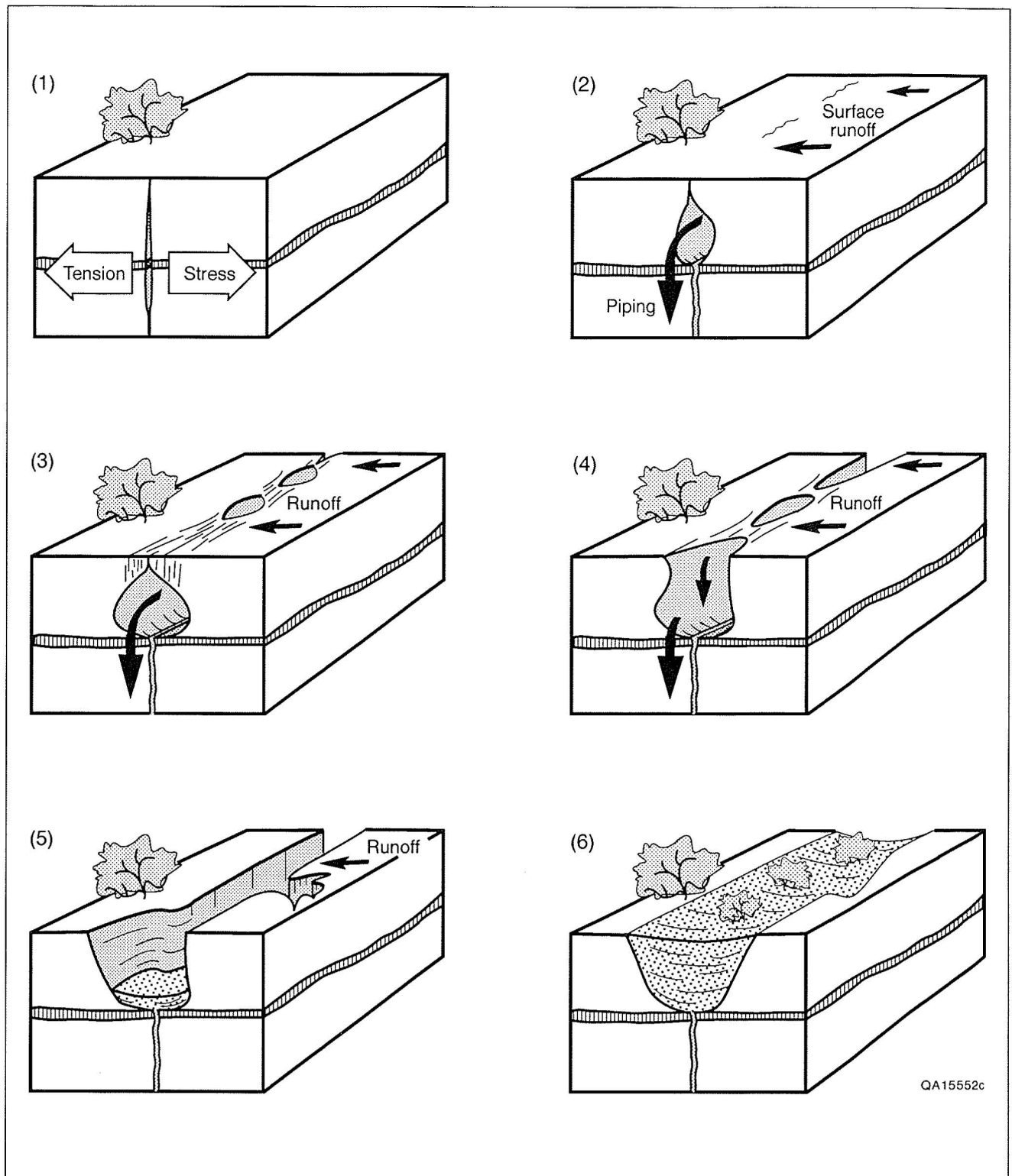
Only four wells within 8 km of the fissures have been described (Leggat, 1962; Davis, 1965). All were drilled in 1960, 18 yr after the 1942 photographs reveal that fissures were already present. Three wells were abandoned by 1965, and the fourth is 4 km from the fissures. It is doubtful that any of these wells affected development of the younger fissures.

Discussion of Natural Fissure Development

Summary of Model

Larson and Péwé (1986) proposed that fissures form above precursor tension fractures in the shallow subsurface (fig. 16). Their model outlines progressive stages of development: (1) initially, a fracture forms in the shallow subsurface and provides a pathway for water moving downward from the surface (fig. 16, stage 1); (2) erosion enlarges the fracture and creates a soil pipe (fig. 16, stage 2); (3) sediments overlying the pipe collapse into the cavity, leaving holes at the surface that directly capture runoff and transported sediment (fig. 16, stage 3); (4) the holes lengthen as they are further eroded by captured runoff, and connect to form a laterally continuous

fissure (fig. 16, stage 4); (5) eventually, the outlet of the soil pipe becomes plugged and the fissure begins to fill with sediment (fig. 16, stage 5); and (6) finally, the fissure fills completely with sediment. As long as a depression remains above the filled fissure, it will preferentially collect and store moisture, providing better growing conditions for woody vegetation, especially deep-rooted phreatophytes such as mesquite (fig. 16, stage 6). At the time of this investigation (1989), the surface fissures in the Hueco Bolson study area were at stage 3 or 4, as shown in figure 16. The relict fracture had developed past stage 6 because it was no longer marked by aligned vegetation or by a topographic low at the surface. The surface fissure there had been destroyed by subsequent erosion and deposition.



QA15552c

FIGURE 16. Block diagrams depicting fissure evolution. After Larson and Péwé (1986, their fig. 7). Sequence: (1) Tensional stress induces fracturing. (2) Runoff enters surface fracture, widening it by erosion. Water moves laterally along the fracture, eroding a soil pipe, and moves downward into the fracture. Base of fissure is at top of carbonate-cemented layer. (3) Surface fractures are enlarged by erosion, surface-collapse features form, and collapse-related fractures form above cavity before unconsolidated material falls into hole. (4) Surface-collapse features capture more runoff and erode laterally. (5) Surface-collapse features coalesce, forming a linear fissure, and fracture fills with sediment. (6) Fracture and fissure fill with sediment. Vegetation along the fissure trace is more vigorous because of greater availability of water.

Tensional Stress and Localization of Fractures

Tensional stress is commonly proposed as the force that causes fracture formation (Bull, 1972; Bouwer, 1977; Holzer and others, 1979; Jachens and Holzer, 1979, 1982; Bell, 1981; Larson and Péwé, 1986). Vertical fractures form at points of maximum horizontal tensile stress (Larson, 1986). Differential subsidence of sediments is typically inferred as the cause of the stress (Larson, 1986). Subsidence is most often attributed to withdrawal of ground water for agricultural or municipal use. For example, fissures have developed in Arizona and California where ground-water levels have declined from 25 to 140 m (table 1) (Holzer, 1976; Morton, 1977; Guacci, 1979; Bell, 1981; Holzer and Pampeyan, 1981; Boling, 1986; Larson, 1986; Larson and Péwé, 1986; Schumann and others, 1986). Other processes that can produce fractures are not as common as differential subsidence in desert basins of the southwestern United States (Larson and Péwé, 1986). These processes include (1) tectonic movements, (2) desiccation of expansive clay soils, and (3) hydrocompaction of low-density sediments.

Nevertheless, desiccation of clay soils cannot be ruled out entirely at the Hueco Bolson study area. Sand-filled desiccation fractures up to 15 cm wide are present in some outcrops of the Fort Hancock Formation (Gustavson, 1991b). A relatively thin alluvial cover with carbonate-cemented horizons to provide rigidity could be fractured by stress transmitted upward from the underlying, contracting clay.

Differential subsidence and the fissures that result may be localized by different geological environments (fig. 17): (1) buried bedrock hills, (2) buried faults or bedrock escarpments, (3) hinge lines between subsiding and stable areas, and (4) buried facies boundaries (Larson, 1986; Larson and Péwé, 1986). Jachens and Holzer (1979) found that earth fissures in alluvium near exposed bedrock are spatially associated with gravity and magnetic anomalies ranging from local highs to convex-upward changes in slope. Most of these inferred bedrock irregularities were at depths less than 250 m. The same study did not detect anomalies beneath fissures that were more than 2 km from bedrock outcrops (Jachens and Holzer, 1979). The fissures in the Hueco Bolson study area are more than 2 km from the nearest bedrock outcrop.

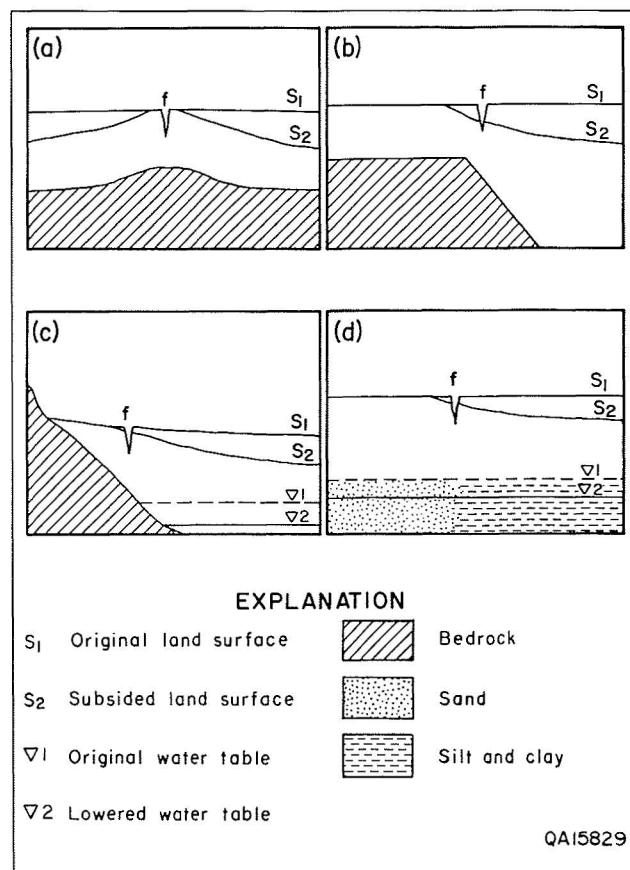


FIGURE 17. Geologic settings of potential fissure development: (a) buried bedrock hill, (b) buried bedrock escarpment, (c) hinge line over boundary of water-table decline, which intersects bedrock slope, and (d) sedimentary facies boundary. Clay desiccation is not limited to any of these settings.

Boling (1986) described the setting of earth fissures in south-central Arizona. Typical fissures are located on alluvial plains between basin centers and adjacent uplifted mountain blocks. The fissures overlie inferred basin-bounding faults or are between the faults and adjacent mountain blocks. The basins are filled with deposits of unconsolidated alluvium, anhydrite, and indurated conglomerate ranging from 50 to 300 m thick.

Conditions similar to those described in south-central Arizona by Boling (1986) prevail at the Hueco Bolson study area (fig. 1b). The study area is located on an alluvial plain between the center of the Rio Grande valley and the Diablo Plateau. It is upslope from the basin-bounding Campo Grande fault. Depth to Cretaceous bedrock ranges from

170 to 220 m, which is within the range of depths reported by Boling (1986). However, despite these similarities, it is uncertain whether relief on buried Cretaceous bedrock is affecting the development or location of the fissures in the study area. There is a small, shallow, closed basin in Cretaceous bedrock beneath the study area (fig. 10), but the relief around the perimeter of this basin may be insufficient to produce tension fractures at the surface.

The Hueco Bolson study area has been crossed by two different seismic reflection surveys, interpreted by Phillips and others (1986) and by Baker and Keller (1990). Phillips and his coworkers (1986) inferred two high-angle faults beneath the study area, whereas Baker and Keller (1990), using data with higher resolution, inferred two low-relief highs on Cretaceous bedrock at about the same locations. Compaction of bolson sediments over these structures may have generated the tensional stress that led to the formation of subsurface fractures and surface fissures. Larson and Péwé (1986) suggested that differential compaction over a bedrock hill produced tensional stress that eventually led to fracture and fissure formation in northeast Phoenix, Arizona. However, four factors suggest that this effect may not have been strong enough to produce the fractures and fissures in the Hueco Bolson study area. First, the depth to the (presumed) bedrock hill beneath the fissures in northeast Phoenix (45 m) is less than one-fourth the depth to Cretaceous bedrock beneath fissure 1 in the Hueco Bolson study area (about 200 m on the basis of core from a borehole about 800 m to the southeast). The inferred bedrock high beneath the Hueco Bolson study area may be too deeply buried for associated differential compaction to have had any effect on near-surface sediments. Second, the inferred bedrock high near fissure 1 has only about half the relief of the buried bedrock hill described by Larson and Péwé (1986) (30 m). The effect of differential subsidence above a smaller structure would be less. Third, fissures 1 and 3 and the relict fracture do not have consistent orientations or positions relative to these subsurface structures (fissure 2 is outside the area where seismic data were collected). Fourth, no significant pumping or drawdown of ground water has occurred at the Hueco Bolson study area, whereas at the Arizona site examined by Larson and Péwé, water levels had declined 90 m since about 1950 (table 1).

Because water levels have not been lowered by pumping in the vicinity of the study area, the fissures there must be attributed to natural phenomena.

Natural water-table lowering has occurred over geologic time. The water table in basin-fill sediments in the Rio Grande Valley has been lowered by incision of the Rio Grande and dewatering of sediments above the lower base level (Gile and others, 1981). Water level in the vicinity of the Campo Grande fault may have been as much as 30 m higher before Rio Grande incision (Mullican and Senger, 1990). The last episode of incision of the Rio Grande occurred more than 10,000 yr ago, and drainage of adjacent permeable basin fill was probably relatively rapid (Gile and others, 1981). Incision of streams to form arroyos upstream from the Campo Grande fault would have had a similar effect on the water table beneath the study area, because sediments higher than the lowered streambeds were drained. In addition, ground-water levels in the study area may be anomalously low (110 to 180 m below ground surface) because of more permeable bolson sediments (Mullican and Senger, 1990). A map of hydraulic head (fig. 18) shows an elongated zone of lower head extending across the northern half of the study area. This has been attributed to preferential drainage of these relatively permeable bolson-fill sediments (Mullican and Senger, 1990). A change to a warmer, drier climate about 8,000 yr ago (Van Devender and Spaulding, 1979) may have contributed to lowering hydraulic heads in the recent geologic past by reducing recharge to the bolson aquifers. Thus, four factors may have combined to lower ground-water levels in the study area over geologic time: incision of the Rio Grande, fault movement on the Campo Grande fault, preferential drainage of relatively permeable basin-fill beneath the study area, and change to a warmer, drier climate.

Natural ground-water lowering eventually would have resulted in compaction of unconsolidated sediment. Differential compaction may have been localized over a bedrock high or around the margins of the bedrock basin beneath the study area. This compaction would have produced extensional stress. Alternatively, more compressible, finer grained sediments nearer the center of the Hueco Bolson may have compacted more than the coarser grained proximal fan sediments near the basin margins where the study area is located. However, stratigraphic information in the study area does not allow us to determine whether a facies boundary such as this lies beneath the fissures.

Similar hydrologic and geologic conditions may prevail in nearby drainage basins where there has been little pumping of ground water and where

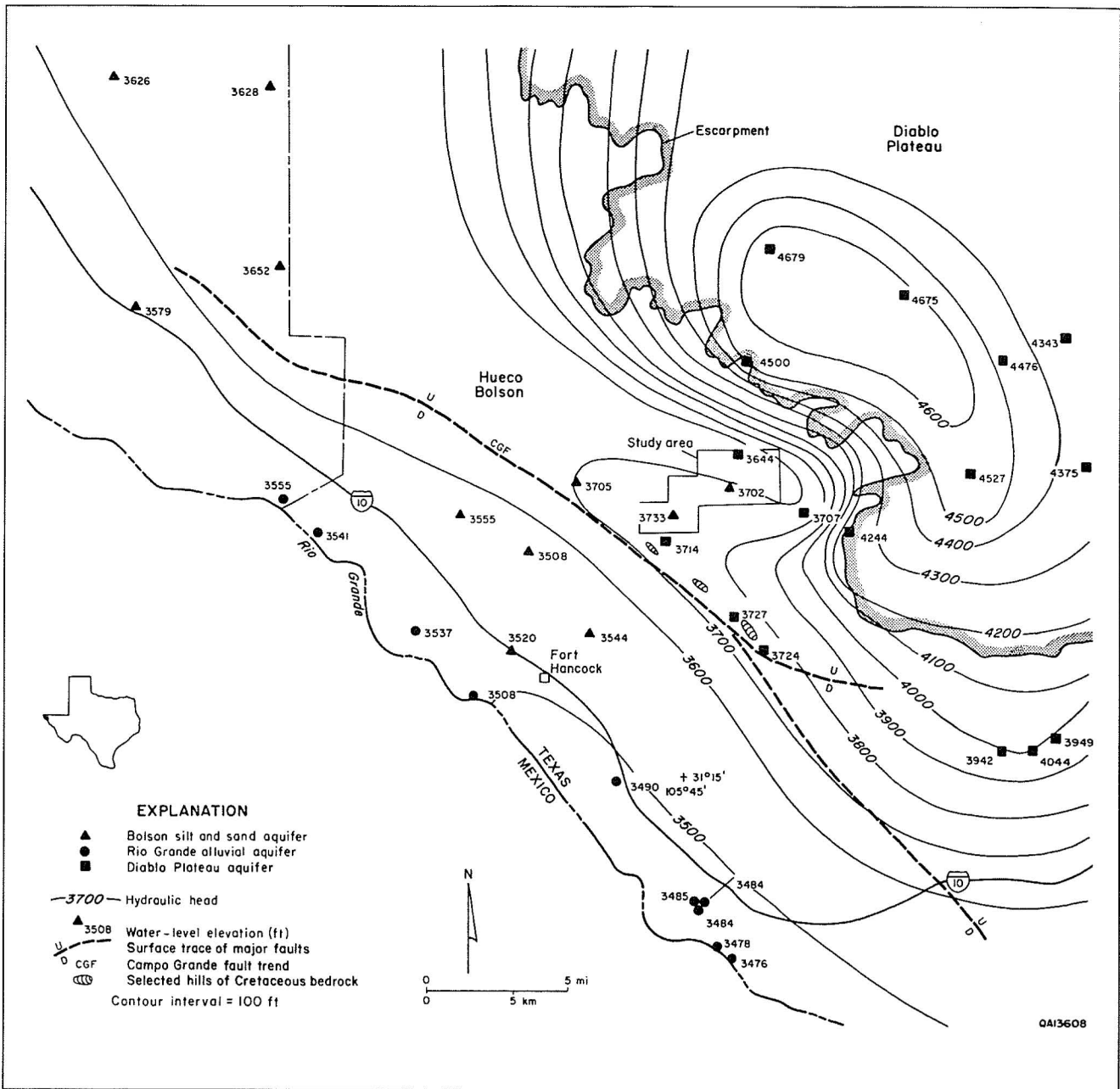


FIGURE 18. Potentiometric surface map of southeastern Hueco Bolson. A zone of lower hydraulic head extends across the northern half of the study area, including locations of the fissures. After Mullican and Senger (1990, their fig. 18).

fissures have existed for at least 65 yr. Fissures at Eagle Flat, Hueco Tanks, Quitman Canyon, Ryan Flat, and Wildhorse Flat form polygonal or branching networks. Sustained desiccation of clayey surface or near-surface sediments in some areas may explain the appearance of polygonal fissures. Several factors (amount of water-table lowering, alluvium thickness, and clay content of near-surface sediments) may

influence development of polygonal fissure networks. Although the fissures at the study area are not polygonal or branching, they may be the first components of a polygonal system that is just beginning to form. The thickness and locally shallow burial of the clay-rich Fort Hancock Formation suggest that clay desiccation may play a part in development of fissures at the study area.

Soil Piping

The principal mechanism in the development of a fissure is erosion that enlarges a preexisting crack at the surface and causes soil piping (fig. 16). According to Cooke and Warren (1973), Parker (1963) identified four conditions that are necessary for soil piping to occur: (1) sufficient water to saturate part of the sediments above base level, (2) hydraulic-head gradient to drive subterranean water movement, (3) permeable and erodible soil above local base level, and (4) an outlet for flow. In the Hueco Bolson study area, surface water is present for only a short time after rain. No perennial streams or springs exist there. Thus, conditions 1 and 2 exist only locally and temporarily after rainstorms in ephemeral stream channels and other low areas. The third condition, permeable and erodible soil, is fulfilled everywhere in the study area except possibly on gravelly outcrops. Local and temporary base level may be at the bottom of this soil on top of the upper calcrete (0.5 to 3 m below the ground surface) (figs. 5 and 6). During and after heavy rains, water may move down preexisting tension fractures, which are common in the study area, and collect on top of the calcrete until it is removed by transpiration or until it moves down through cracks in the petrocalcic horizon. Chloride data from the vicinity of the fissure indicate that water has moved downward through the profile, at least to the top of the upper calcrete. But these data may not reflect the localized effects of small fractures on downward water movement. Potential paths for flow out of the fissure (the fourth condition mentioned previously) also exist in the Hueco Bolson study area. Water may simply flow into deeper parts of the fracture, or it may flow into the permeable grain-supported gravel that underlies the upper calcrete (figs. 5 and 6). Altogether, the four conditions necessary for piping to occur along fractures in the Hueco Bolson study area probably exist only locally in topographic lows and temporarily during and after heavy rains.

Surface Collapse

Overland flow contributes to formation and enlargement of collapse features that form the fissure at the surface. This condition has been recorded in reports on fissures in Arizona (Leonard, 1929; Holzer, 1976; Boling, 1986), California (Morton,

1977; Guacci, 1979), and Texas (Underwood and DeFord, 1975). Many fissures are nearly perpendicular to local drainage, suggesting that capture of overland flow is an important factor in their enlargement. But, this effect is secondary—their location and orientation are primarily controlled by a preexisting tension fracture.

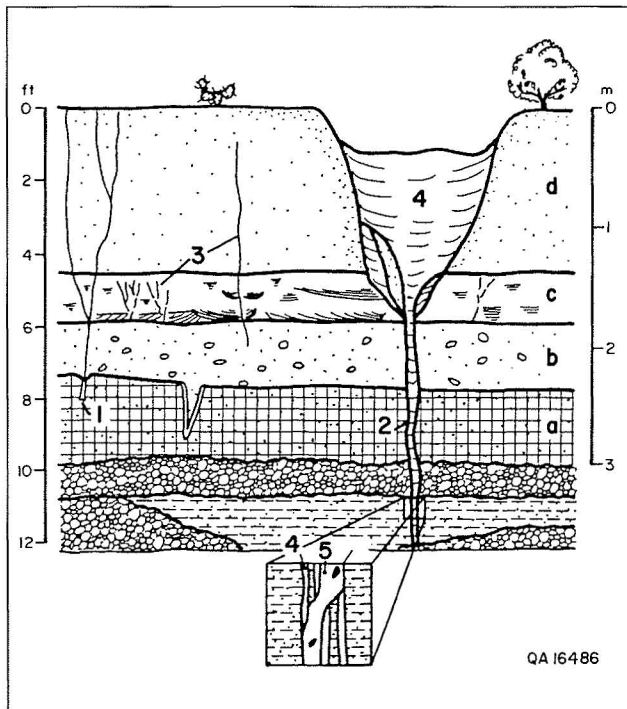
Summary of Fissure Development

The origin of tensional stress that caused the fractures in the Hueco Bolson study area to form may be differential compaction of unconsolidated sediments. Bedrock structure (fig. 10) may enable the tensional stress caused by compaction to form fractures in near-surface sediments. Not all tension cracks that formed in the petrocalcic horizon (fig. 19, no. 1) became precursors to the fissure. The fractures that did develop fissures propagated to the surface probably within about the last 20 yr and began to capture runoff (fig. 19, no. 2). Other fractures formed, which did not become precursors to fissures (fig. 19, no. 3). No fault movement has occurred along the fractures.

Water introduced by overland flow eroded the tension crack at the surface, enlarging it and resulting in collapse of surface sediments into the fissure (fig. 19, no. 4). More tensional fracturing or desiccation of fill produced subvertical fractures in the fracture fill that were later lined with clay laminae (fig. 19, no. 5).

On the basis of aerial photographs taken in 1971 and 1985, collapse features at fissure 1 are inferred to have formed between 1971 (photographic scale 1:16,000) and 1985 (approximate scale 1:14,000). No collapse features are visible on the 1971 photographs, but they are present on the 1985 photographs. Although fissure 1 is visible, collapse features at fissures 2 and 3 cannot be seen on the most recent photographs (1989, scale 1:5,000), so their age is undetermined. No surface-collapse features appear at the relict fracture.

Fissure 1 appears to be older and at a more mature stage of development than fissures 2 and 3. Fissures 2 and 3 will probably follow similar patterns of development, although they may develop slower because they are in smaller drainage basins. Overland flow will continue to enlarge the fissures until the outlet for sediment is plugged; then they will fill



with sediment. This process may take many decades to complete. Fissures that were open in 1924 in Quitman Canyon, southeast of the study area, are still open today, and adjacent sediments are still collapsing into them.

FIGURE 19. Schematic cross section of fissure 1. Development of the fissure is discussed in the text (p. 36). Symbols: (a) Stage III to IV petrocalcic horizon, (b) poorly sorted, massive gravelly sand, (c) crossbedded sand, (d) structureless silty sand, (1) fracture in petrocalcic horizon, (2) tension fracture, precursor to fissure, (3) other fractures, which may be caused by trenching, (4) sediment filling surface-collapse feature and (inset) fracture, and (5) fabric resulting from episodic fracture filling.

Summary and Conclusions

The surface of the study area in the Hueco Bolson is composed primarily of low-relief interfluvial and drainageways of ephemeral streams. Strata underlying the area and cropping out locally are the Tertiary Fort Hancock and Tertiary-Quaternary Camp Rice Formations and younger Quaternary strata. The older formations are composed primarily of interbedded sand, silt, and clay and have local concentrations of gravel. Expansive clay soils that have local desiccation cracks are present in the Fort Hancock Formation. The younger Quaternary sediments have less clay and more gravel than the two older formations.

Three surface fissures, which resulted from surface collapse and piping along preexisting tension fractures, are present in the study area. The surface-collapse features are aligned in discontinuous, curvilinear segments that overlap locally. All three surface fissures are in local topographic lows, which indicates that concentrated overland flow is an essential component in their development. A relict fracture, with no surface fissure above it, has been exposed in a 6-m-deep trench and is not now in a topographic low but may have been in the past. The surface-collapse features that developed over it

have been removed by subsequent erosion and deposition.

Tension fractures are typically 2 to 4 cm wide where they have not been widened by erosion or slumping. Parallel symmetry of opposite walls of the fractures is common. The fractures extend at least 6 m deep below ground surface. Internal clay laminae within fracture-filling sediment represent multiple filling events and may indicate more than one episode of fracture opening.

The source of tensional stress that formed the tension fractures is unknown. Similar fractures in similar settings in Arizona and California have been attributed to differential compaction of unconsolidated sediments over bedrock irregularities. Compaction is commonly attributed to pumping of ground water. Although there has been no significant ground-water withdrawal in the study area, ground-water levels have been lowered naturally and unevenly over geologic time. Bedrock irregularities beneath the study area are buried deeper and have less local relief than those reported at other fissure sites, but they may have enough relief to generate tensional stress in overlying sediments.

Fissures are present in nearby basins where ground-water pumping has not been as extensive as it has been in Arizona and California. In addition, fissures have formed before inception of ground-water withdrawal in some basins. The polygonal morphology of these fissures suggests that

desiccation of near-surface clays may contribute to their development. Thus, fissure development appears to be a natural geomorphic phenomenon in arid desert basins that have undergone climate change and ground-water lowering since the Quaternary.

Acknowledgments

Funding for this work was provided by the Texas Low-Level Radioactive Waste Disposal Authority under interagency contract number IAC(90-91)0268. Conclusions of the authors are not necessarily approved or endorsed by the Authority. The authors wish to acknowledge the assistance and cooperation of the staff of the Texas Low-Level Radioactive Waste Disposal Authority in Fort Hancock, Texas, who facilitated field work. Jeffrey N. Rubin assisted with collection of field data. Billy Copeland, Cruz Gomez, Butch Hickox, and Juan Villalobos excavated and cleaned trenches. We extend our special thanks to Deron Kasparian of Valentine, Texas, who provided considerable assistance, insightful observations, and a delicious lunch during our tenure in Valentine. Mark Baker and Duncan Moss, of the Department

of Geological Sciences at The University of Texas at El Paso, shared their insights and data on fissures at Valentine and near Hueco Tanks.

Consultations with Edward W. Collins, Mary Gillam, Thomas C. Gustavson, Jay A. Raney, and Richard H. Raymond, and reviews by Raney, Gustavson, Arten J. Avakian, Alan R. Dutton, and Robert Mace improved the quality of the circular. Figures were drafted by Wade W. Kolb, Joel L. Lardon, Yves Oberlin, Patrice A. Porter, Maria Saenz, and Tari Weaver under the direction of Richard L. Dillon, chief cartographer. Tucker F. Hentz was technical editor. Others contributing to the report were Susan Lloyd, word processing and typesetting, Bobby Duncan, editing, and Jamie H. Coggin, design.

References

- Albritton, C. C., Jr., and Smith, J. R., Jr., 1965, Geology of the Sierra Blanca area, Hudspeth County, Texas: U.S. Geological Survey Professional Paper 479, 131 p.
- Allen, B. L., 1990, Soils of the Texas Low-Level Radioactive Waste Disposal Authority site study area: Texas Tech University, Department of Agriculture, Horticulture, and Entomology, report prepared for the Texas Low-Level Radioactive Waste Disposal Authority, 12 p.
- Baker, C. L., 1927, Exploratory geology of a part of southwestern Trans-Pecos Texas: University of Texas, Austin, Bureau of Economic Geology Bulletin 2745, 70 p.
- Baker, Mark, and Keller, G. R., 1990, Seismic reflection survey for the proposed low-level radioactive waste repository, Hudspeth County, Texas, in Keller, G. R., Doser, D. I., and Baker, Mark, Geophysical studies related to the proposed low-level radioactive waste repository, Hudspeth County, Texas: The University of Texas at Austin, Bureau of Economic Geology, report prepared for the Texas Low-Level Radioactive Waste Disposal Authority under contract number IAC(90-91)0268, 63 p.
- Bell, J. W., 1981, Subsidence in Las Vegas valley: Mackay School of Mines, University of Nevada, Reno, Bureau of Mines and Geology Bulletin 95, 84 p.
- Boling, J. K., 1986, Earth-fissure movements in south-central Arizona, U.S.A., in Johnson, A. I., Carbognin, L., and Ubertini, L., eds., Land subsidence: Proceedings of the Third International Symposium on Land Subsidence, Venice, Italy, March 19-25, 1984, International Association of Hydrological Sciences Publication No. 151, p. 757-766.
- Bouwer, Herman, 1977, Land subsidence and cracking due to ground-water depletion: *Ground Water*, v. 15, no. 5, p. 358-364.
- Bull, W. B., 1972, Prehistoric near-surface subsidence cracks in western Fresno County, California: U.S. Geological Survey Professional Paper 437-C, 85 p.

- Collins, E. W., and Raney, J. A., 1991, Neotectonic history and structural style of the Campo Grande fault, Hueco Basin, Trans-Pecos Texas: The University of Texas at Austin, Bureau of Economic Geology Report of Investigations No. 196, 39 p.
- Contaldo, G. J., and Mueller, J. E., 1988, Earth fissures in the Deming area, in Mack, G. H., Lawton, T. F., and Lucas, S. G., eds., Cretaceous and Laramide tectonic evolution of southwestern New Mexico: New Mexico Geological Society 39th Annual Field Conference, Guidebook, p. 3-5.
- Cooke, R. U., and Warren, Andrew, 1973, Geomorphology in deserts: Berkeley, California, University of California Press, 374 p.
- Davis, M. E., 1965, Development of ground water in the El Paso District, Texas, 1960-63, Progress Report No. 9: Texas Water Commission Bulletin 6514, 34 p.
- Dirección General de Geografía, 1981, Carta geológica, Chihuahua, Estados Unidos Mexicanos: scale 1:1,000,000.
- 1982, Carta geológica San Antonio el Bravo, Estados Unidos Mexicanos: Map 13-5, scale 1:250,000.
- Folk, R. L., 1974, Petrology of sedimentary rocks: Austin, Texas, Hemphill Publishing Company, 182 p.
- Gile, L. H., Hawley, J. W., and Grossman, R. B., 1981, Soils and geomorphology in the Basin and Range area of Southern New Mexico—Guidebook to the desert project: New Mexico Bureau of Mines and Mineral Resources, Memoir 39, 222 p.
- Goetz, L. K., 1977, Quaternary faulting in Salt Basin Graben, West Texas: The University of Texas at Austin, Master's thesis, 136 p.
- 1985, Giant polygonal desiccation cracks in Wildhorse Flat, West Texas—revisited, in Dickerson, P. W., and Muehlberger, W. R., eds., Structure and tectonics of Trans-Pecos Texas: West Texas Geological Society Publication 85-81, p. 235-238.
- Guacci, Gary, 1979, The Pixley fissure, San Joaquin Valley, California, in Saxena, S. K., ed., Evaluation and prediction of subsidence: International Conference on Evaluation and Prediction of Subsidence, Pensacola Beach, Florida, January 1978, American Society of Civil Engineers, p. 303-319.
- Gustavson, T. C., 1991a, Arid basin depositional systems and paleosols: Fort Hancock and Camp Rice Formations (Pliocene-Pleistocene), Hueco Bolson, West Texas and adjacent Mexico: The University of Texas at Austin, Bureau of Economic Geology Report of Investigations No. 198, 49 p.
- 1991b, Buried Vertisols in lacustrine facies of the Pliocene Fort Hancock Formation, Hueco Bolson, West Texas and Chihuahua, Mexico: Geological Society of America Bulletin, v. 103, no. 4, p. 448-460.
- Haenggi, W. T., 1966, Geology of El Cuervo area, northeastern Chihuahua, Mexico: University of Texas, Austin, Ph.D. dissertation, 403 p.
- Hall, S. A., 1985, Quaternary pollen analysis and vegetational history of the Southwest, in Bryant, V. M., Jr., and Holloway, R. G., eds., Pollen records of Late-Quaternary North American sediments: Dallas, Texas, American Association of Stratigraphic Palynologists, p. 95-123.
- Haneberg, W. C., Reynolds, C. B., and Reynolds, I. B., in press, Monoclinial flexure of surficial strata and the origin of an earth fissure near San Marcial, New Mexico: Journal of Geophysical Research.
- Hawley, J. W., and Kottowski, F. E., 1969, Quaternary geology of the south-central New Mexico border region, in Kottowski, F. E., and LeMone, D. V., eds., Border Stratigraphy Symposium, 1968, El Paso, Texas: New Mexico Bureau of Mines and Mineral Resources, Circular 104, p. 89-115.
- Henry, C. D., Gluck, J. K., and Bockoven, N. T., compilers, 1985, Tectonic map of the Basin and Range province of Texas and adjacent Mexico: The University of Texas at Austin, Bureau of Economic Geology Miscellaneous Map No. 36, scale 1:500,000.
- Holzer, T. L., 1976, Ground failure in areas of subsidence due to ground-water decline in the United States, in Land subsidence: Proceedings of the Second International Symposium on Land Subsidence, Anaheim, California, December 13-17, 1976, International Association of Hydrological Sciences Publication No. 121, p. 423-433.
- Holzer, T. L., Davis, S. N., and Lofgren, B. E., 1979, Faulting caused by groundwater extraction in southcentral Arizona: Journal of Geophysical Research, v. 84, no. B2, p. 603-612.
- Holzer, T. L., and Pampeyan, E. H., 1981, Earth fissures and localized differential subsidence: Water Resources Research, v. 17, no. 1, p. 223-227.
- Horowitz, A., Gerald, R. E., and Chaiffetz, M. S., 1981, Preliminary paleoenvironmental implications of pollen analyzed from Archaic, Formative, and Historic sites near El Paso, Texas: The Texas Journal of Science, v. 33, no. 1, p. 61-72.
- Jachens, R. C., and Holzer, T. L., 1979, Geophysical investigations of ground failure related to ground-water withdrawal—Picacho Basin, Arizona: Ground Water, v. 17, no. 6, p. 574-585.
- 1982, Differential compaction mechanism for earth fissures near Casa Grande, Arizona: Geological Society of America Bulletin, v. 93, no. 10, p. 998-1012.
- Keller, G. R., 1990, Regional geophysics and gravity survey in the vicinity of the proposed low-level radioactive waste repository, Hudspeth County, Texas, in Keller, G. R., Doser, D. I., and Baker, Mark, Geophysical studies related to the proposed low-level radioactive waste repository, Hudspeth County, Texas: The University of Texas at Austin, Bureau of Economic Geology, report prepared for the Texas Low-Level Radioactive Waste Disposal Authority under contract number IAC(90-91)0268, p. 47-63.
- Larson, M. K., 1986, Potential for subsidence fissuring in the Phoenix, Arizona, U.S.A. area, in Johnson, A. I., Carbognin, L., and Ubertini, L., eds., Land subsidence: Proceedings of the Third International Symposium on Land Subsidence, Venice, Italy, March 19-25, 1984, International Association of Hydrological Sciences Publication No. 151, p. 291-299.
- Larson, M. K., and Péwé, T. L., 1986, Origin of land subsidence and earth fissuring, northeast Phoenix, Arizona:

- Association of Engineering Geologists Bulletin, v. 23, no. 2, p. 139-165.
- Leggat, E. R., 1962, Development of ground water in the El Paso District, Texas, 1955-60, Progress Report No. 8: Texas Water Commission Bulletin 6204, 56 p.
- Leonard, R. J., 1929, An earth fissure in southern Arizona: *Journal of Geology*, v. 37, no. 8, p. 765-774.
- Long, C. A., and Killingley, C. A., 1983, The badgers of the world: Springfield, Illinois, Charles C. Thomas, 404 p.
- Machette, M. N., 1985, Calcic soils of the southwestern United States, in Weide, D. L., ed., *Soils and Quaternary geology of the southwestern United States*, Geological Society of America Special Paper 203, p. 1-21.
- Markgraf, Vera, Bradbury, J. P., Forester, R. M., Singh, G., and Sternberg, R. S., 1984, San Agustin Plains, New Mexico: age and paleoenvironmental potential reassessed: *Quaternary Research*, v. 22, p. 336-343.
- McFadden, L. D., and Tinsley, J. C., 1985, Rate and depth of pedogenic-carbonate accumulation in soils: formulation and testing of a compartment model, in Weide, D. L., ed., *Soils and Quaternary geology of the southwestern United States*, Geological Society of America Special Paper 203, p. 23-41.
- Morton, D. M., 1977, Surface deformation in part of the San Jacinto Valley, southern California: U.S. Geological Survey *Journal of Research*, v. 5, no. 1, p. 117-124.
- Mullican, W. F., III, and Senger, R. K., 1990, Hydrologic characterization of ground-water resources in south-central Hudspeth County, Texas: The University of Texas at Austin, Bureau of Economic Geology, report prepared for the Texas Low-Level Radioactive Waste Disposal Authority under contract number IAC(90-91)0268, 88 p.
- Parker, G. G., 1963, Piping, a geomorphic agent in landform development of the drylands: *International Association of Scientific Hydrology Publication* 65, p. 103-113.
- Phillips, J. D., Dean, D. F., and Riherd, P. S., 1986, Preliminary seismic reflection study of the Fort Hancock area in Hudspeth County, Texas: The University of Texas at Austin, Institute for Geophysics, report prepared for the Texas Low-Level Radioactive Waste Disposal Authority under contract number IAC(86-87)0994, UTIG Technical Report TR-45, 44 p.
- Raney, J. A., and Collins, E. W., 1990, Regional geologic setting of the Fort Hancock study area, Hudspeth County, Texas: The University of Texas at Austin, Bureau of Economic Geology, report prepared for the Texas Low-Level Radioactive Waste Disposal Authority under contract number IAC(90-91)0268, 69 p.
- Reeves, C. C., Jr., 1976, Caliche—origin, classification, morphology and use: Lubbock, Texas, Estacado Books, 233 p.
- Robinson, G. M., and Peterson, D. E., 1962, Notes on earth fissures in southern Arizona: U.S. Geological Survey Circular 466, 7 p.
- Scanlon, B. R., Richter, B. C., and Wang, F. P., 1991, Field studies and numerical modeling of unsaturated flow in the Chihuahuan Desert, Texas: The University of Texas at Austin, Bureau of Economic Geology Report of Investigations No. 199, 56 p.
- Scanlon, B. R., Wang, F. P., and Richter, B. C., 1990, Analysis of unsaturated flow based on physical data related to low-level radioactive waste disposal, Chihuahuan Desert, Texas: The University of Texas at Austin, Bureau of Economic Geology, report prepared for the Texas Low-Level Radioactive Waste Disposal Authority under contract number IAC(90-91)0268, 102 p.
- Schumann, H. H., Cripe, L. S., and Laney, R. L., 1986, Land subsidence and earth fissures caused by groundwater depletion in southern Arizona, U.S.A., in Johnson, A. I., Carbognin, L., and Ubertini, L., eds., *Land subsidence: Proceedings of the Third International Symposium on Land Subsidence*, Venice, Italy, March 19-25, 1984, International Association of Hydrological Sciences Publication No. 151, p. 841-851.
- Schumann, H. H., and Poland, J. F., 1970, Land subsidence, earth fissures and groundwater withdrawal in south-central Arizona, U.S.A., in *Land subsidence: Proceedings of the International Symposium on Land Subsidence*, Tokyo, Japan, September 1969, International Association of Hydrological Sciences Publication No. 88, v. 1, p. 295-302.
- Sellards, E. H., 1932, The Valentine, Texas, earthquake, in *Contributions to Geology, 1932: University of Texas*, Austin, Bureau of Economic Geology Bulletin 3201, p. 113-138.
- Sergent, Hauskins and Beckwith, Consulting Geotechnical Engineers, 1989, Preliminary geologic and hydrologic evaluation of the Fort Hancock site (NTP-S34), Hudspeth County, Texas, for the disposal of low-level radioactive waste: report prepared for Hudspeth County, Texas, Hudspeth County Conservation and Reclamation District No. 1, Hudspeth County Underground Water Conservation District No. 1, El Paso County, Texas, SHB Job No. 388-4008B, v. 1 and 2.
- Slaff, Steven, 1989, Patterns of earth-fissure development: examples from Picacho Basin, Pinal County, Arizona: *Arizona Geology*, v. 19, no. 3, p. 4-5.
- Underwood, J. R., Jr., and DeFord, R. K., 1969, Large-scale desiccation fissures in alluvium, Trans-Pecos Texas and northern Chihuahua (abs.): *Geological Society of America, Abstracts with Programs*, v. 1, pt. 2, p. 31.
- , 1975, Large-scale desiccation fissures in alluvium, Eagle Mountain area, in *Geology of the Eagle Mountains and vicinity, Trans-Pecos Texas: Society of Economic Paleontologists and Mineralogists, Permian Basin Section Guidebook*, Publication 75-15, p. 135-139.
- Van Devender, T. R., and Spaulding, W. G., 1979, Development of vegetation and climate in the southwestern United States: *Science*, v. 204, p. 701-710.
- White, D. E., Gates, J. S., Smith, J. T., and Fry, B. J., 1980, Ground-water data for the Salt Basin, Eagle Flat, Red Light Draw, Green River Valley, and Presidio Bolson in westernmost Texas: Texas Department of Water Resources Report 259, 97 p.